CHAPTER IV

RESULTS AND DISCUSSION

4.1 Characterization of raw materials

Particle size distribution of raw clay was measured as shown in Fig. 4.1. The average size of particle is about 2.6 μm and the highest wt.% of amount is the particle size of about 4 μm. Hence high plasticity of red clay was thought to come from these fine particles.

4.1.1 Particle size distribution

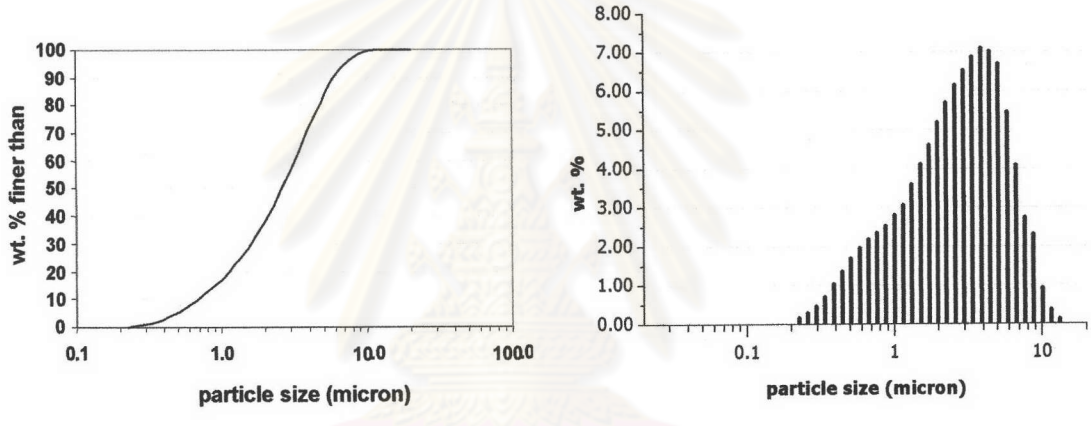

(a) (b)

Fig. 4.1. Particle size distribution of clay dissolved in water with dispersant, hexa-meta-phosphoric acid 0.2 wt.% solution, (a) accumulated curve, (b) histogram.

Particle size distributions of sand and grog were measured as shown in Fig. 4.2. Most of sand particles are coarse. Around 90 wt.% of sand particles are in the range of 150-850 μm and about 37.7 wt.% are in the range of 300-500 μm.

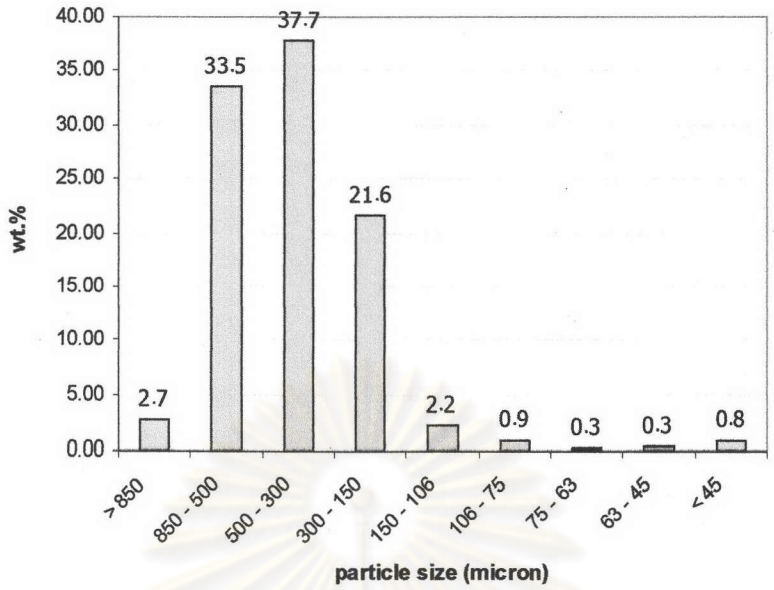

Fig. 4.2. Particle size distribution of sand.

The particle size of grog is finer than that of sand particles as shown in Fig. 4.3. Around 60 wt.% of grog particles are in the range of 150-850 μm, and about 24.9 wt.% are in the range of 500-850 μm. Grog contains 13.0 wt% of particles less than 45 μm. However, grog also contains 11.4 wt% of particles over 850 μm. These values are much more than that of sand (2.7 wt%). As a result grog includes both coarse and fine particles, while sand is mainly composed of coarse particles.

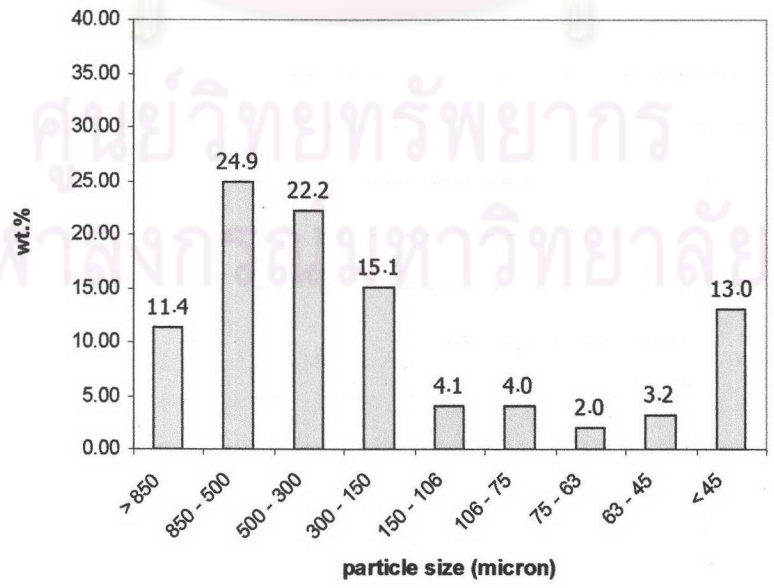

Fig. 4.3. Particle size distribution of grog.

4.1.2 Water content

Water contents in raw materials are shown in Fig. 4.4. Plastic forming method is used in real production because of the high plasticity of raw clay. The water content in clay after adding water for plastic kneading was 21 ± 2 wt.%.

Water content of sand comes from wet sieving process. And then, it is stocked on the yard outdoors. Water content of grog comes from adsorbed moisture in ambient air.

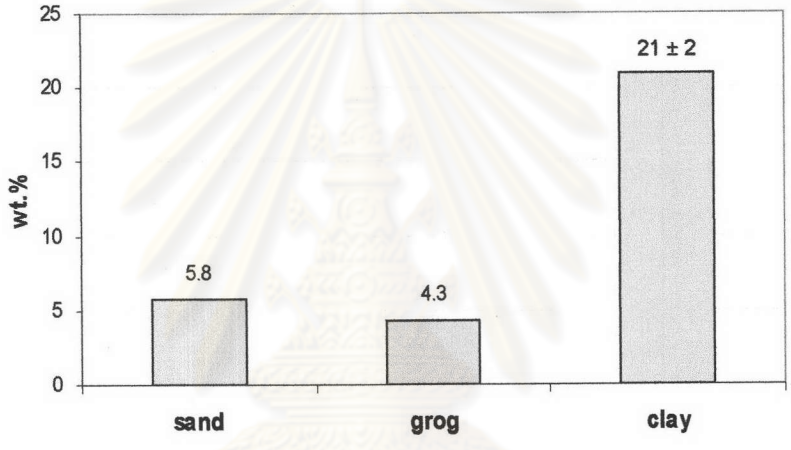

Fig. 4.4. Water content in raw materials.

4.1.3 Chemical composition

Table 4.1shows the chemical composition of raw clay and glass powder. The chemical composition of raw clay is typical of a kaolinite-based material with low amounts of alkali oxides and high percentage of SiO_2 and Al_2O_3. This confirms the low density after sintering at low temperature. The high percentage of Fe_2O_3 in raw clay is responsible for the orange-red color of the product and specimen after firing.

The chemical composition of the glass powder is typical of soda-lime glass which contains large amount of SiO_2, CaO and Na_2O. The high percentage of alkali and alkaline earth oxides is responsible for the high efficiency as fluxing material.

Low percentage of Fe_2O_3 ensures that there will be no effect to fired color of product and specimen and is a good reason to select this material.

Table 4.1. Chemical composition of clay and glass powder.

raw materials	Oxide compositions (wt. %)									
	SiO_2	Al_2O_3	Fe_2O_3	TiO_2	CaO	MgO	K_2O	Na_2O	other	LOI.
clay	62.07	21.47	3.63	0.88	0.50	0.65	1.24	0.36	1.00	8.21
glass powder	68.00	1.18	0.09	-	11.20	1.00	0.21	17.85	0.47	-

4.1.4 Crystal phase

Fig. 4.5 shows the XRD patterns of the raw clay. The XRD profile indicates that the clay is predominantly kaolinite-based clay with the presence of much amount of quartz and muscovite (potassium mica, $KAl_2(Si_3Al)O_{10}(OH)_2$). Quartz is the main phase and the broad peaks indicate imperfect crystalline materials.

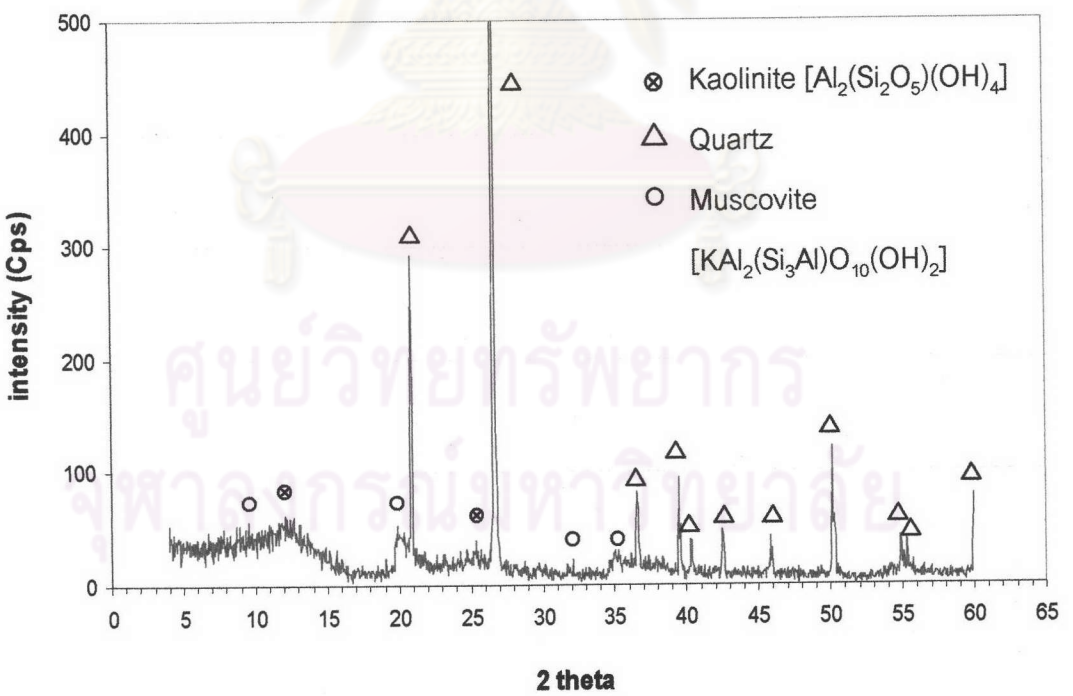

Fig. 4.5. Crystal phase analyzed of raw clay.

4.2 Characterization of commercial products

The properties of commercial terra-cotta product of Siamese Merchandise Co., Ltd. (SM 1, SM 2), Portugal and German were comparatively characterized.

4.2.1 Water absorption and bulk density

Fig. 4.6 shows the water absorption of commercial products. Fig. 4.6 (a) shows the average water absorption of each commercial product. The water absorption of SM 1 (top diameter = 19 cm) is about 14% but SM 2 (top diameter = 32 cm) is higher and close to 15%. The SM 1 and SM 2 are composed of the same material but high water absorption in bigger size may come from two reasons. One is the lower pressure than that of smaller size products in roller press forming. The second is the setting position of products in the furnace. Because most of bigger size pottery was arranged under smaller size one. And the temperature at the bottom side was a little lower than the top side in the furnace.

The water absorption of Portugal product and German product are 13.4% and 9.7%, respectively. These values are lower than those of SM products.

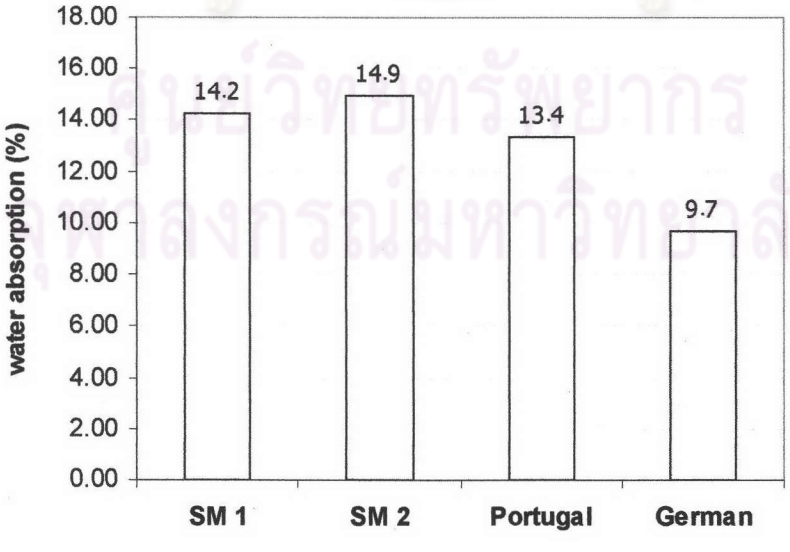

(a)

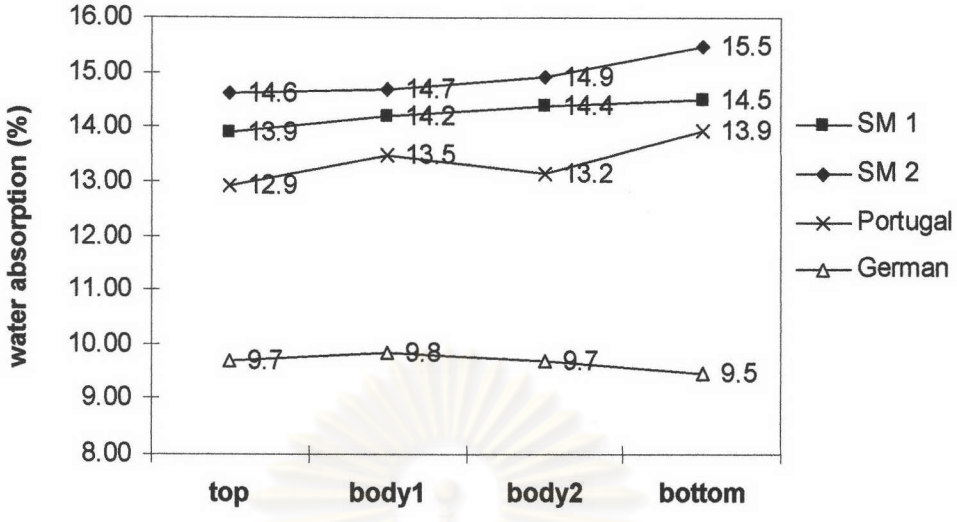

(b)

Fig. 4.6. Water absorption of commercial terra-cotta products (a) average water absorption (b) each part of products (SM = Siamese Merchandise Co.,Ltd., 1=small size (top diameter = 19 cm), 2=large size (top diameter = 32 cm)).

The commercial products were cut in four parts and water absorption was measured as shows in Fig. 4.6 (b). The first part called "top" is the ring of the top rim of pottery. The second part was called "body1" is the upper half of body. The third part called "body2" is the under half of body. The last part called "bottom" is the bottom part of pottery.

Water absorption of commercial products, SM 1, SM 2 and Portugal, increase from top to bottom. On the other hand, water absorption of German product decreases from top to bottom. One factor which affects the amount of water absorption is the thickness of products. In SM 1, SM 2 and Portugal, the thickness of the bottom is a little thicker. In German product, the relation is reverse.

Fig. 4.7 (a) shows average bulk density of commercial products. Bulk density of pottery is in a reverse order with water absorption. Low water absorption means high bulk density. German product has the highest bulk density of 2.12 g/cm^3 and SM products have the lowest bulk density conforming with its water absorption. The bulk density of Portugal product is a little higher than that of SM 2 but is the same value as SM 1.

Fig. 4.7 (b) shows bulk density in each part of products. German product has very high bulk density in each part and increases from top to bottom conforming with its water absorption which decreases from top to bottom. And bulk densities of both SM and Portugal products decrease from top to bottom.

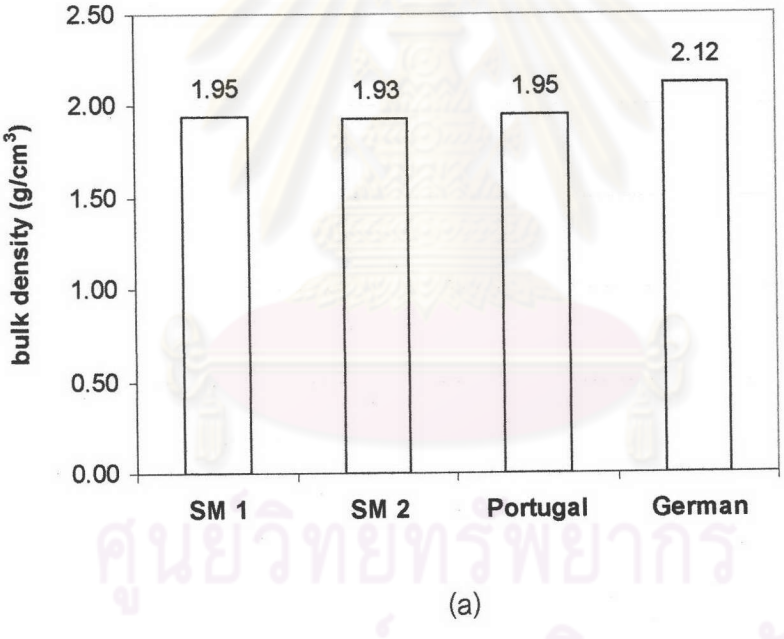

(a)

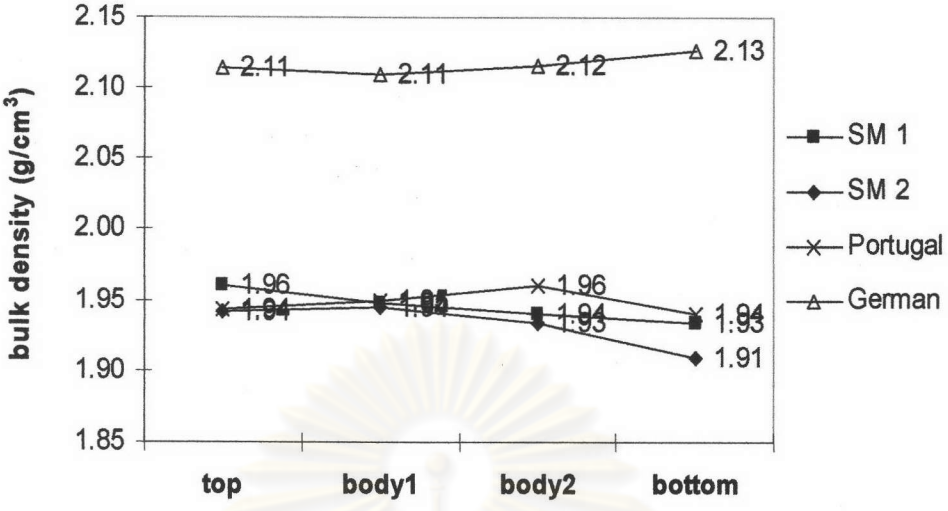

(b)

Fig. 4.7. Bulk density of commercial products (a) average bulk density (b) each part of products (SM = Siamese Merchandise Co.,Ltd., 1=small size (top diameter = 19 cm), 2=large size (top diameter = 32 cm)).

4.2.2 Capillary pore volume

Fig. 4.8 shows capillary pore volume (< 2 μm) of commercial products. Because frost damage comes from the freezing of entrapped water in capillary pore, hence the product with low capillary pore volume should have high frost resistance.

Capillary pore volume of German product is very low which suggests high frost resistance. Capillary pore volume of Portugal product is much lower than that of SM 1 and SM 2, but its water absorption shows only small difference. Hence Portugal product is high in macro pore volume but low in capillary pore volume which also suggests high frost resistance. SM products are high in both water absorption and capillary pore volume which lead to low frost resistance.

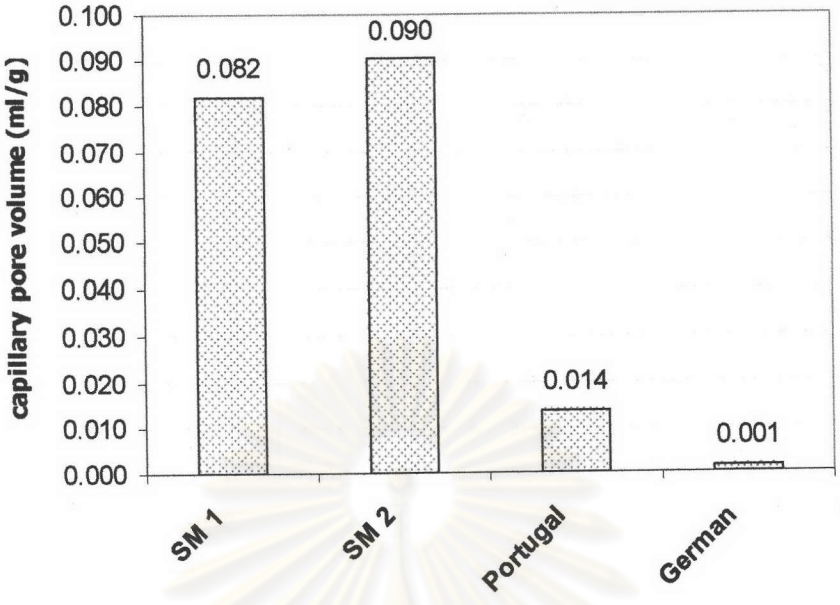

Fig. 4.8. Capillary pore volume (< 2 μm) of SM 1, SM 2, Portugal and German.

4.2.3 Microstructure

Fig. 4.9 shows the microstructures of commercial products. SM product shows coarse sand particles, iron particles and pores in small and large sizes resulted from an ineffective pressing of the forming machine and shrinkage of the mixture components (clay, sand and grog). The pores from an ineffective pressing are aligned along the shear direction of forming and are always generated at the layer boundaries. The shrinkage of the mixture components generates small pores at their boundaries especially when the coarse particles are presented in the body.

A micrograph of the Portugal product shows particle size of sand finer than that of SM product and pores in small size aligned along the shear direction of forming and no porosity at boundaries of the mixture components. German product shows homogeneous distribution of fine sand particles in the body and only fine pores were presented.

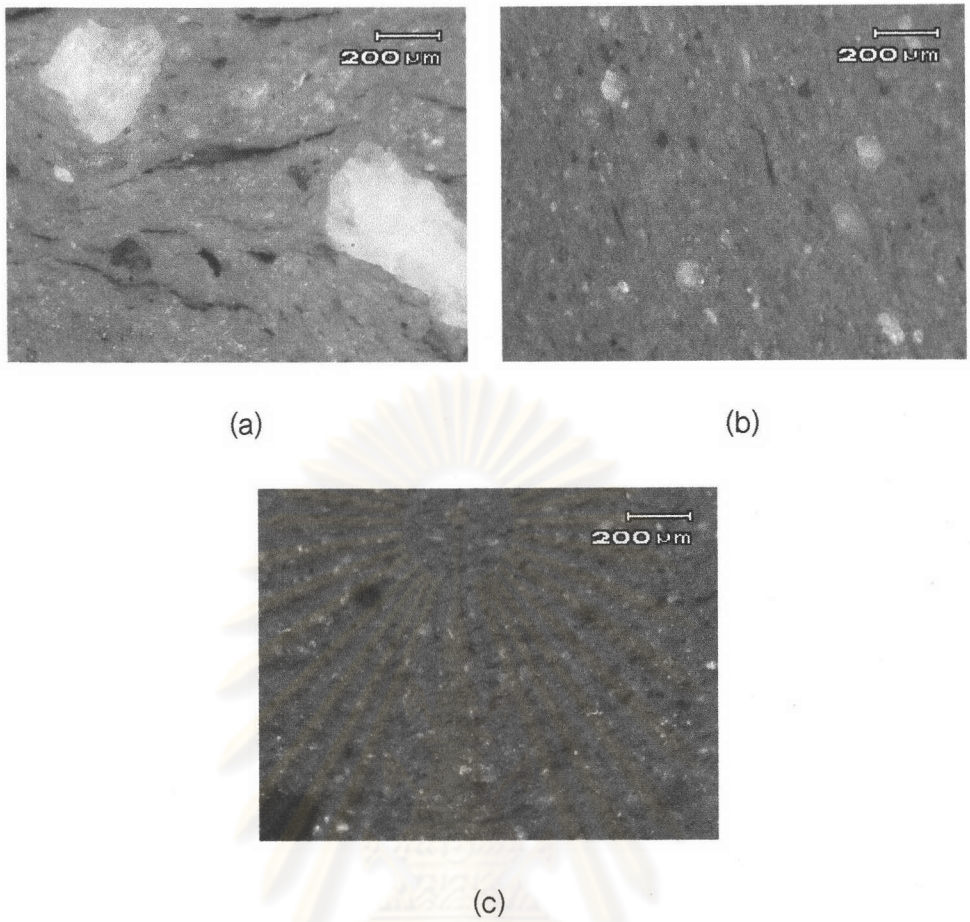

(a) (b)

(c)

Fig. 4.9. Microstructures of commercial products (a) SM, (b) Portugal and (c) German.

4.2.4 Chemical composition

Table 4.2 shows the chemical composition of commercial products. Portugal and German products contain relatively much amount of alkali and alkaline earth oxides in comparison with the SM product. This suggests that the high water absorption and low bulk density in SM products come from the lower amount of alkali and alkaline earth component. High percentage of Fe_2O_3 is the origin of the orange-red color after firing.

Table 4.2. Chemical composition of commercial products.

potteries	Oxide compositions (wt. %)								
	SiO_2	Al_2O_3	Fe_2O_3	TiO_2	CaO	MgO	K_2O	Na_2O	other
SM	71.25	20.86	3.86	0.86	0.44	0.70	1.32	0.36	0.35
Portugal	67.61	21.58	5.14	0.68	0.21	1.10	3.05	0.40	0.23
German	70.49	17.93	5.79	0.93	0.43	0.92	2.22	0.98	0.31

4.2.5 Crystal phase

Fig. 4.10 (a), (b) and (c) show the XRD patterns of SM, Portugal and German commercial products. The XRD patterns of SM and Portugal products show the presence of quartz as the main phase, hematite (Fe_2O_3) and microcline (potassium feldspar, $KAlSi_3O_8$). Both microcline and hematite phases in Portugal product are more intense than in SM product which conform to the high contents of Fe_2O_3 and K_2O in Table 4.2.

Paragonite (sodium mica, $NaAl_3Si_3O_{11}$) can be observed in German product according to its high percentage of Na_2O. However, quartz is still the main phase in German product.

Both microcline and paragonite are the sources of K_2O and Na_2O which act as fluxes to reduce the sintering temperature and accelerate densification.

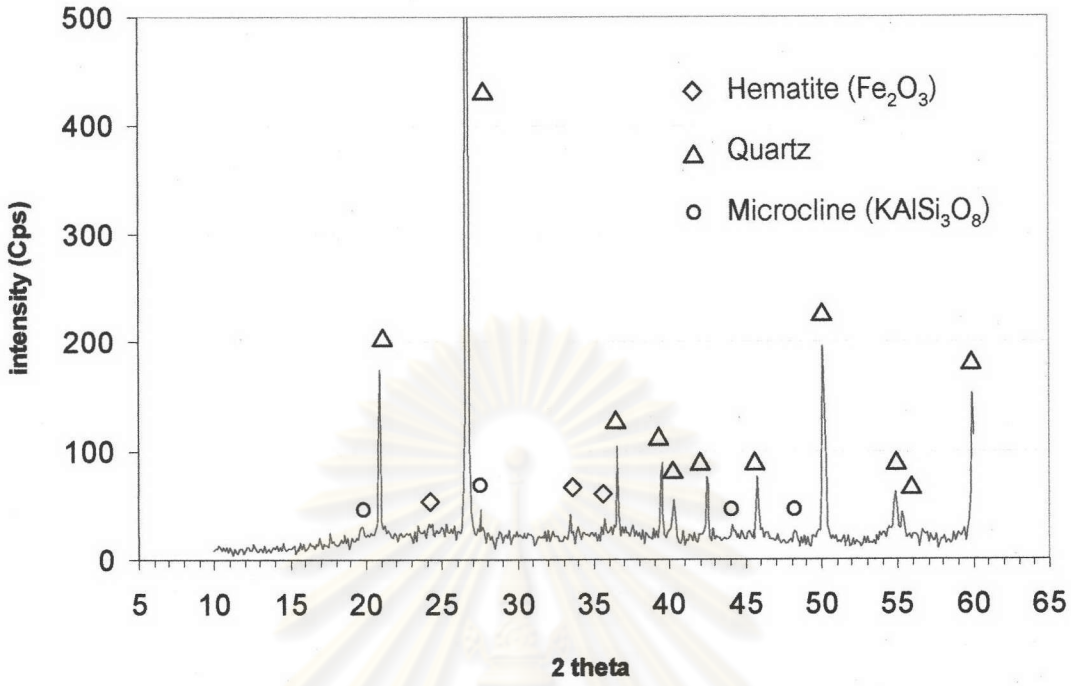

(a) SM commercial product

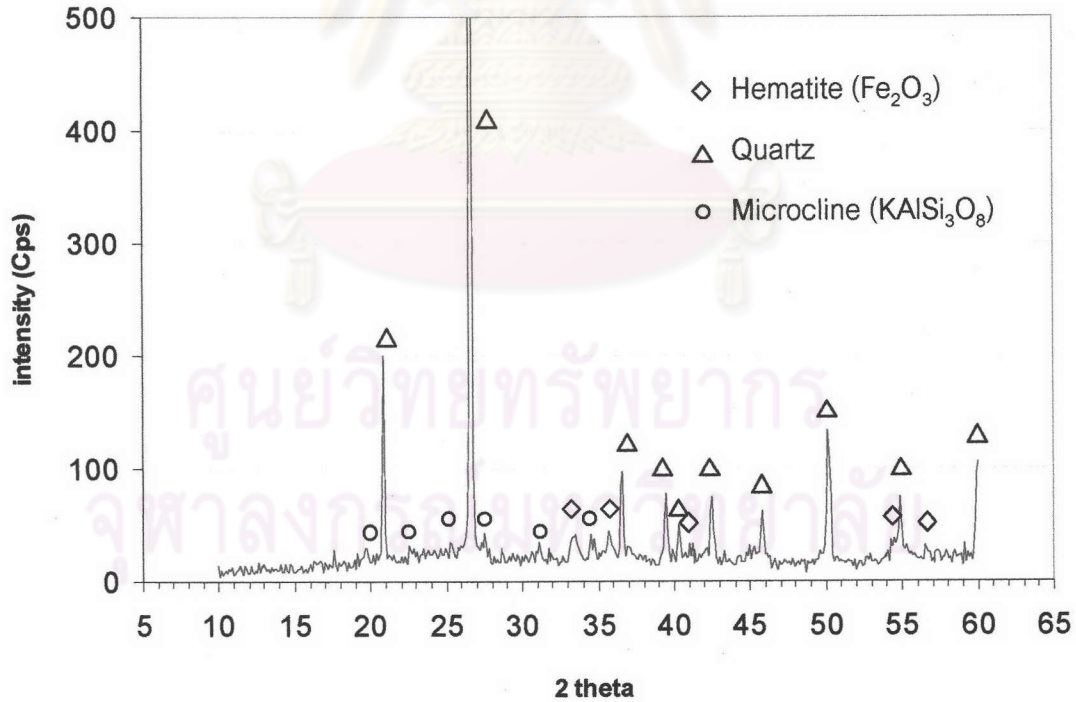

(b) Portugal commercial product

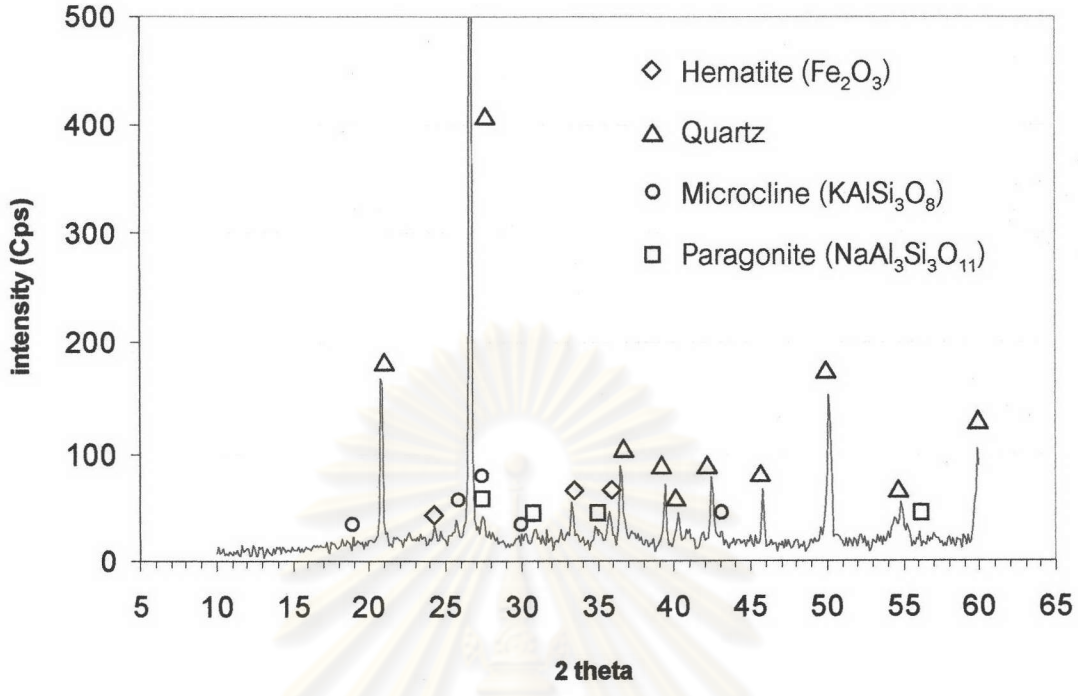

(c) German commercial product

Fig. 4.10. XRD patterns of commercial products (a) SM (b) Portugal (c) German.

4.2.6 Summary

1. German commercial product is lowest in water absorption. Water absorption of Portugal commercial product is lower than that of SM commercial product. SM commercial products are highest in water absorption.

2. Capillary pore volume (< 2 μm) of German product is very low resulted in high frost resistance. SM products are high in water absorption and high volume in capillary pore volume resulted in low frost resistance.

3. Microstructure of SM product shows coarse sand particles and pores. Portugal and German products show finer sand particle and smaller pores than SM product.

4. Portugal and German products contain relatively much amount of alkali and alkaline earth oxides, while SM product has lower amount of alkali and alkaline earth oxides.

5. The XRD patterns of SM, Portugal and German commercial products show quartz as the main phase.

4.3 Effect of amount and particle size of sand and grog

4.3.1 Shrinkage

Shrinkage after drying is shown in Fig. 4.11. The drying shrinkage has a significant relation with the amount and particle size of non-plastic materials such as sand and grog. The drying shrinkage decreases when the amounts of sand or grog increase. It is thought that the coarse particles of sand and grog disturb the shrinkage of clay. The coarse particle size of sand does not affect the shrinkage, on the other hand, fine grog decreases it.

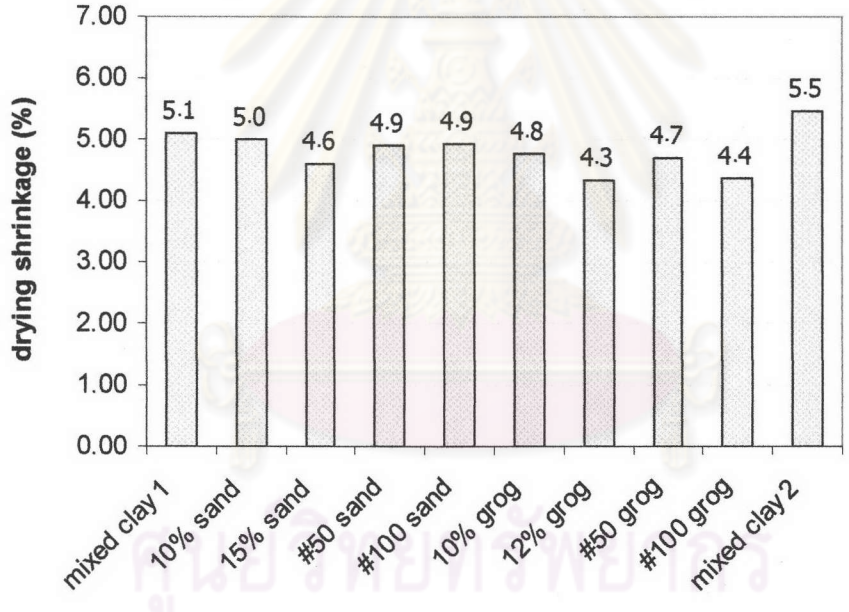

Fig. 4.11. Drying shrinkage of mixed clay (1, 2), sand (10%, 15%, #50 and #100) and grog (10%, 12%, #50 and #100).

Fig. 4.12 shows firing shrinkage of mixed clay (1, 2) and sand (10%, 15%, #50 and #100). These results indicate that firing shrinkage increases with rising temperature. Firing shrinkage decreases obviously at every temperature when the

amount of sand increases because sand particles do not sinter in it self. The effect of particle size of sand is small comparing with that of its amount.

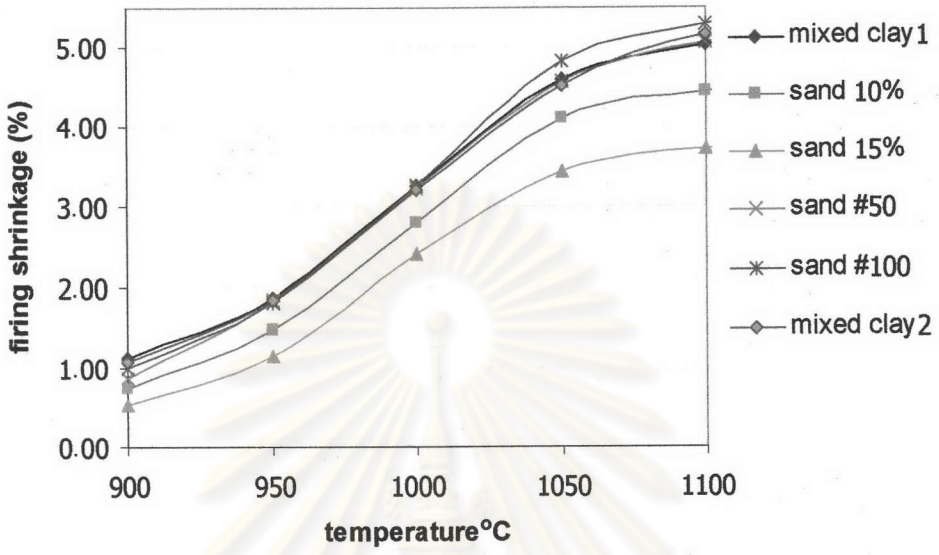

Fig. 4.12. Firing shrinkage of mixed clay (1, 2) and sand (10%, 15%, #50 and #100).

Fig. 4.13 shows firing shrinkage of mixed clay (1, 2) and grog (10%, 12%, #50 and #100). In the case of grog, neither amount nor particle size affects firing shrinkage.

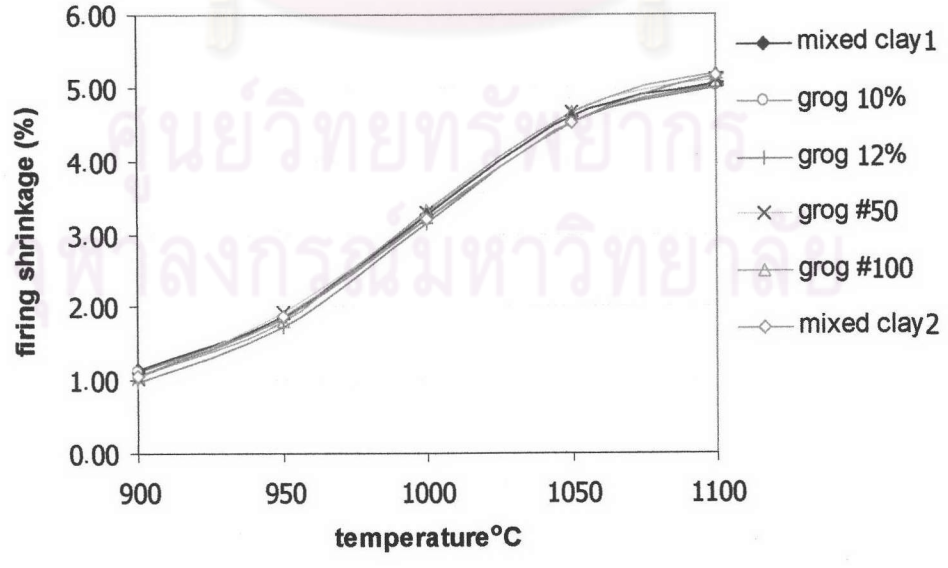

Fig. 4.13. Firing shrinkage of mixed clay (1, 2) and grog (10%, 12%, #50 and #100)

4.3.2 Water absorption and bulk density

Water absorption and bulk density of mixed clay1, sand (10%, 15%, #50, and #100) are shown in Fig. 4.14 (a) and (b). The water absorption decreases and bulk density increases with rising temperature. Water absorption increases but bulk density decreases when the amount of sand increases. Because non-plastic material such as sand increases the open porosity. Water absorptions of mixed clay1, sand 10%, 15%, #50, and #100 are almost the same in the range 900-950°C.

Water absorption can be reduced and bulk density will be increased when the particle size of sand decreases, because fine sand particle does not disturb vitrification. The effect of particle size of sand on water absorption is small comparing with that of its amount.

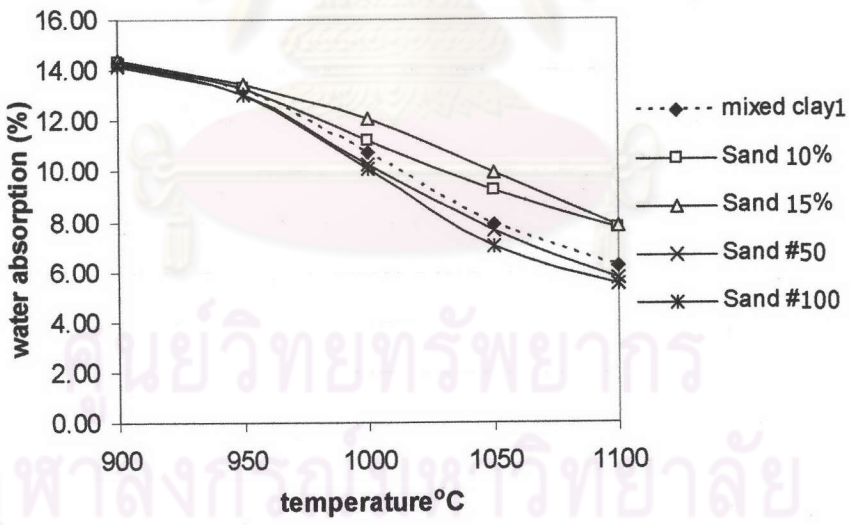

(a)

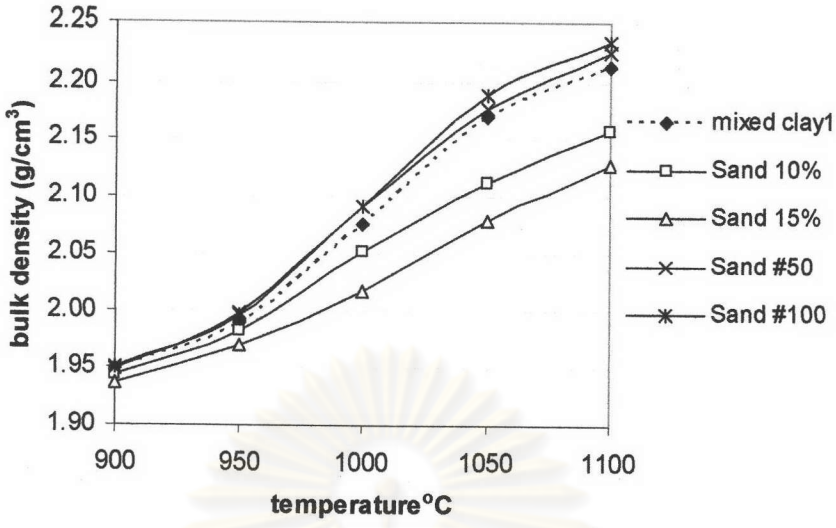

(b)

Fig. 4.14. Water absorption (a) and bulk density (b) of mixed clay1, sand (10%, 15%, #50 and #100).

Fig. 4.15 (a) and (b) show water absorption and bulk density of mixed clay1, Grog (10%, 12%, #50, and #100). In the case of grog, the trends of water absorption and bulk density are the same as that of sand. Water absorption increases but bulk density decreases when the amount of grog increases. But water absorption does not change so much with the amount of grog because grog includes much amount of fine particles.

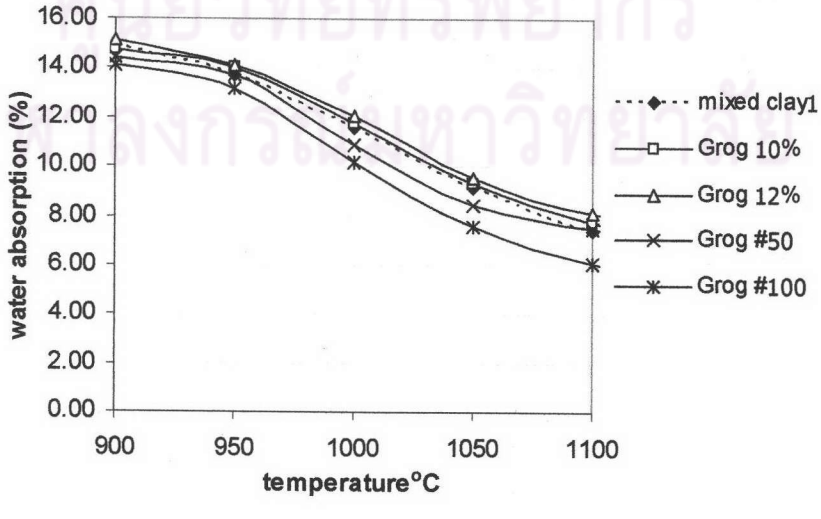

(a)

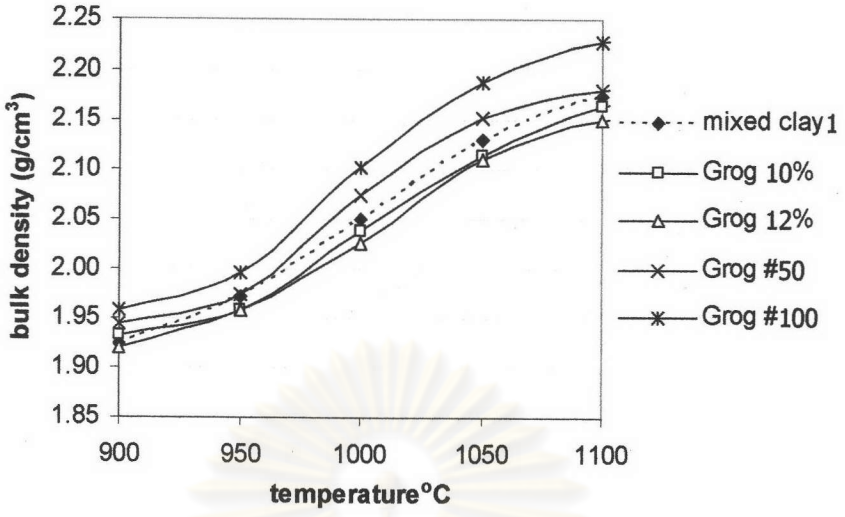

(b)

Fig. 4.15. Water absorption (a) and bulk density (b) of mixed clay1, Grog (10%, 12%, #50 and #100).

Bulk density increases when the particle size of grog is reduced. The effect of particle size of grog on bulk density is larger than that of its amount. This is also due to the chemical inertness of grog.

Fig. 4.16 (a) and (b) are water absorption and bulk density of mixed clay 1 and 2 as a function of firing temperature. The mixed clay 2 includes -50 mesh particle sizes of sand and grog which are smaller than those of mixed clay 1.

Water absorption and bulk density of mixed clay 1 and 2 are almost the same at 900 °C. At 950°C, water absorption of mixed clay1 decreases from 13.3 to 12.6 % of mixed clay2 and bulk density of mixed clay1 increases from 1.99 to 2.00 g/cm^3 of mixed clay2. As the result, water absorption decreases and bulk density increases when the particle size of sand and grog were reduced.

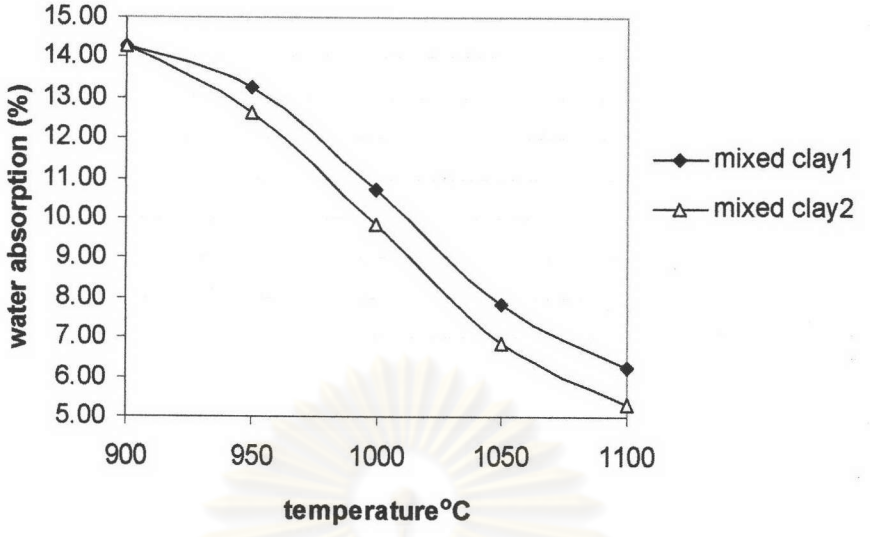

(a)

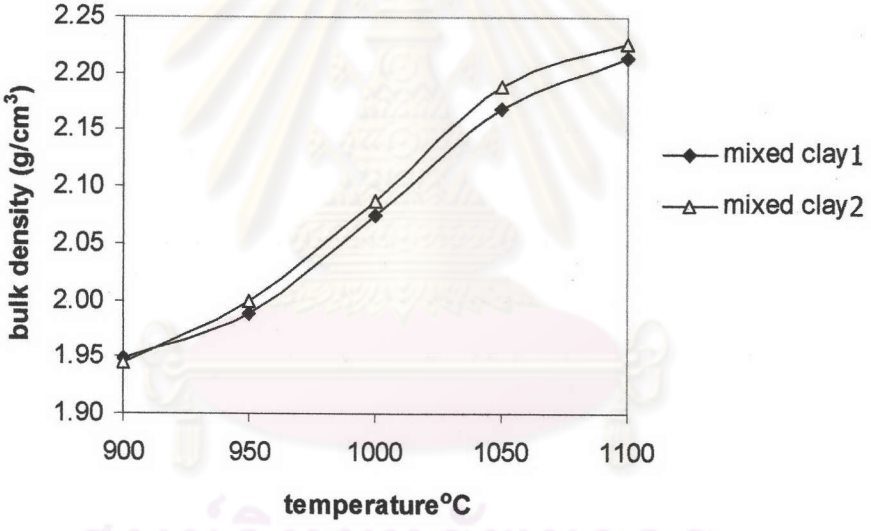

(b)

Fig. 4.16. Water absorption (a) and bulk density (b) of mixed clay 1 and mixed clay 2.

4.3.3 Color

Fig. 4.17 shows fired color of mixed clay 1 specimens at 900-1200°C. Colors of fired specimen vary from orange to purple and dark-brown, depending on the firing temperature. The orange color is produced at low temperature (900°C) and the dark-brown is produced at high temperature (1200°C). The various shades of the red color come from iron oxide (3.6 wt%) in raw clay. Hematite (Fe_2O_3) gives red color but both magnetite (Fe_3O_4) and ferrous oxide (FeO) give black color at all temperatures. The dark-brown color at high temperature comes from the reduction of the red ferric oxide to the black ferrous oxide and the defect in the crystal structure of hematite which increases with temperature. Since the desirable color is orange-red color, the terra-cotta should not be fired over 1000°C.

Fig. 4.17. Fired color of mixed clay 1 at 900-1200°C.

4.3.4 Microstructure

Fig. 4.18 shows cross sectional microstructures of mixed clay 1 specimens. Coarse sand and iron particles are present in mixed clay 1 specimens. The porosity from an ineffective pressing and shrinkage of the mixture components occur inside of the body and increase with rising firing temperature but the porosity in the surface decreases at higher temperature.

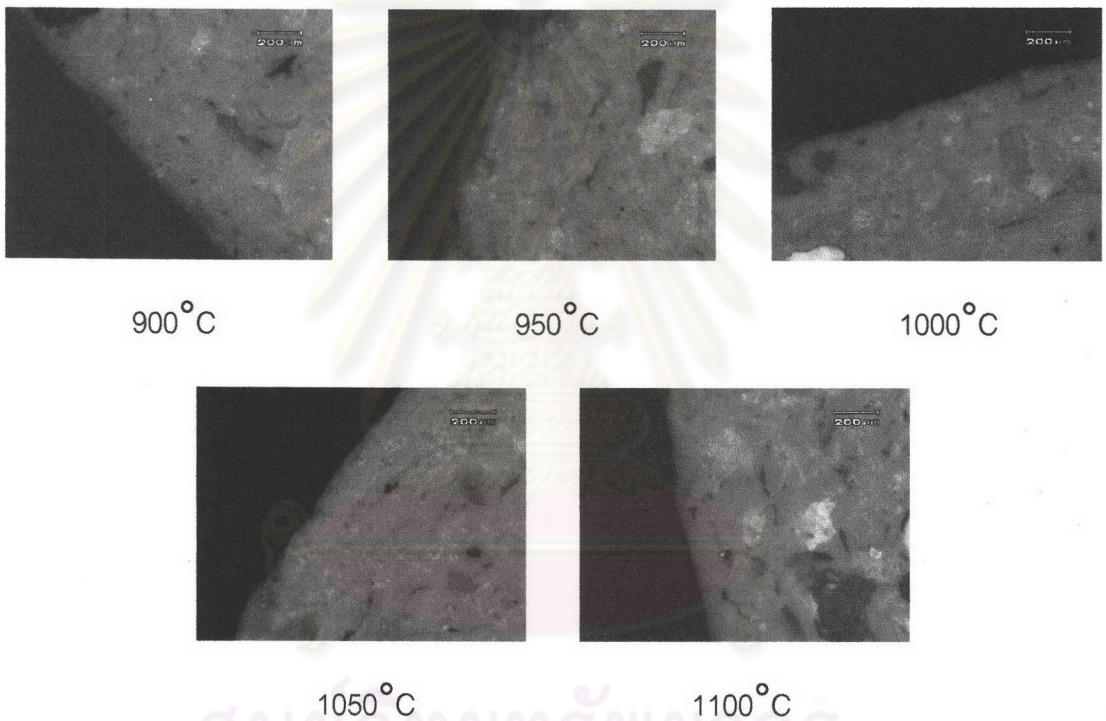

Fig. 4.18. Cross sectional microstructures of mixed clay 1 specimens.

Fig. 4.19 shows cross sectional microstructures of mixed clay 2 specimens. Coarse sand particles were disappeared and replaced by fine sand particles. The porosity from shrinkage of the mixture components decreases but porosity from an ineffective pressing still occurs and increases with rising the firing temperature.

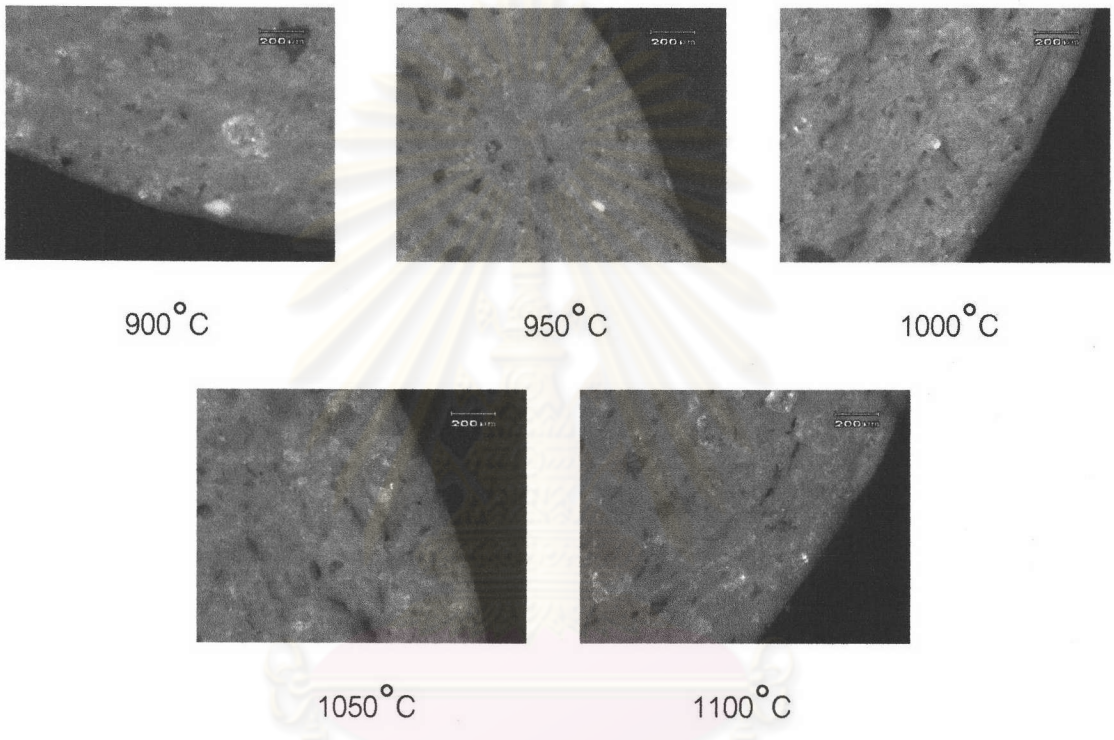

Fig. 4.19. Cross sectional microstructures of mixed clay 2 specimens.

4.3.5 Bending strength

Fig. 4.20 shows three point bending strength of mixed clay1, sand (10%, 15%, 50 mesh and 100 mesh) specimens. Strength increases with the rising of firing temperature and decreases when the amount of sand increases. Bending strength of 15% sand is lower than that of 10% sand and significantly lower than that of mixed clay 1, because the strength comes from the vitrification of clay body. The effect of particle size of sand on bending strength is small comparing with that of its amount. However, the strength of specimens with finer sand increases more than that of the standard (mixed clay 1).

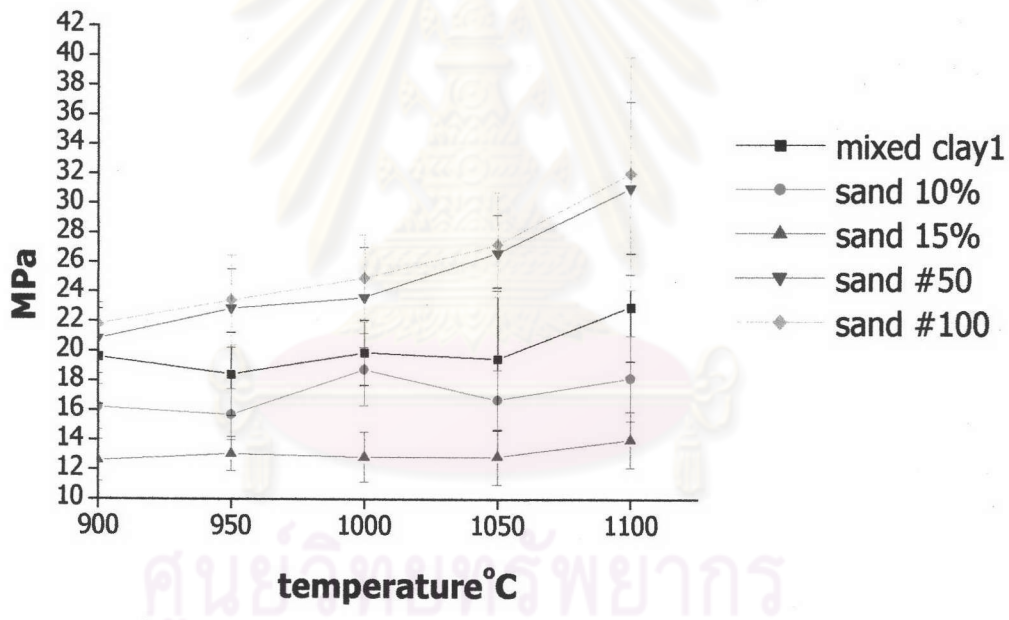

Fig. 4.20. Three point bending strength of mixed clay1, sand (10%, 15%, #50 and #100).

Fig. 4.21 shows three point bending strength of mixed clay1, grog (10%, 12%, 50 mesh and 100 mesh) specimens. Strength increased when the firing temperature increased. Both the amount and particle size of grog do not significantly affect the strength. Strength increases with reducing particle size of grog and decreases with increasing the amount of grog particles.

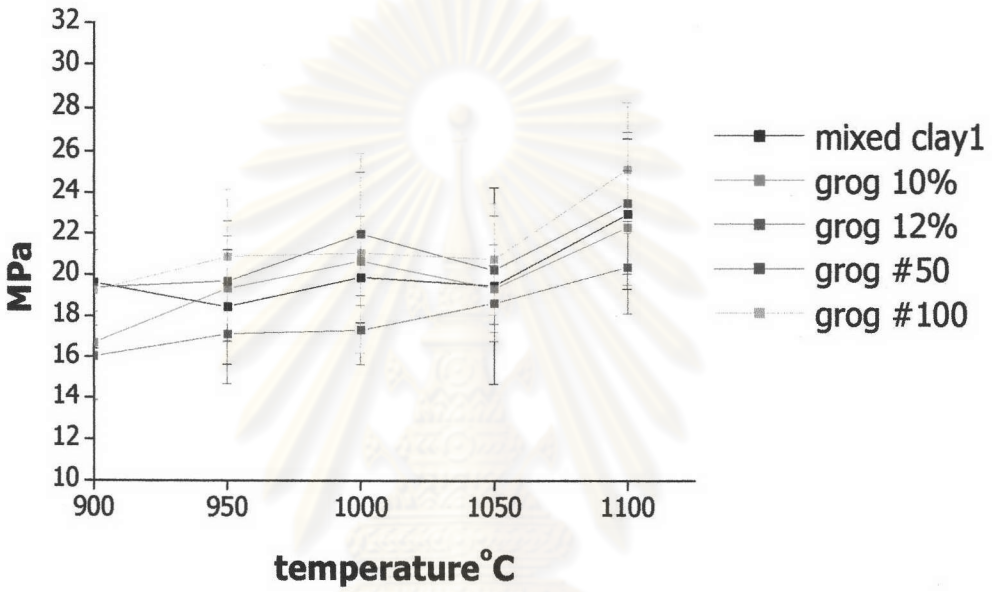

Fig. 4.21. Three point bending strength of mixed clay1, grog (10%, 12%, #50 and #100).

Fig. 4.22 shows three point bending strength of mixed clay 1 and mixed clay 2 specimens. The strength increases with increasing the firing temperature. Bending strength of mixed clay 2 is much higher than that of mixed clay 1 because both the particle sizes of sand and grog reduced to 50 mesh.

Generally strength is controlled by the largest crack in the surface or inside the body. When there are large sizes of sand, they will become the origins of crack. On the other hand, grog is almost the same composition material with mixed clay body. Therefore, the size and amount of grog does not affect the strength as much as sand.

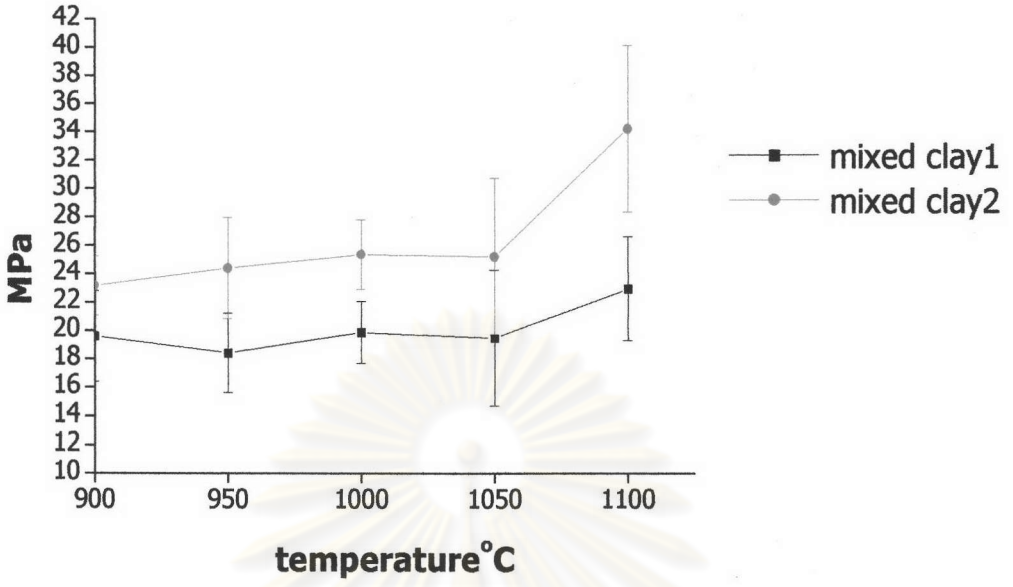

Fig. 4.22. Three point bending strength of mixed clay 1 and mixed clay 2.

4.3.6 Crystal phase

Fig. 4.23 shows XRD patterns of mixed clay 1 fired at 900°C and 1000°C. The XRD pattern of mixed clay 1 shows quartz as the main phase at both temperatures. Microcline (potassium feldspar, $KAlSi_3O_8$) and hematite (Fe_2O_3) are revealed at 900°C. Hematite is the cause of orange color shown in XRD pattern at 900°C and it content decreases at 1000°C. Magnetite phase (Fe_3O_4) resulted from the reduction of ferric oxide is the cause of dark-brown color. Microcline phase decreases at high temperature. Probably potassium in microcline reacts with SiO_2 and Al_2O_3 and formed glassy phase.

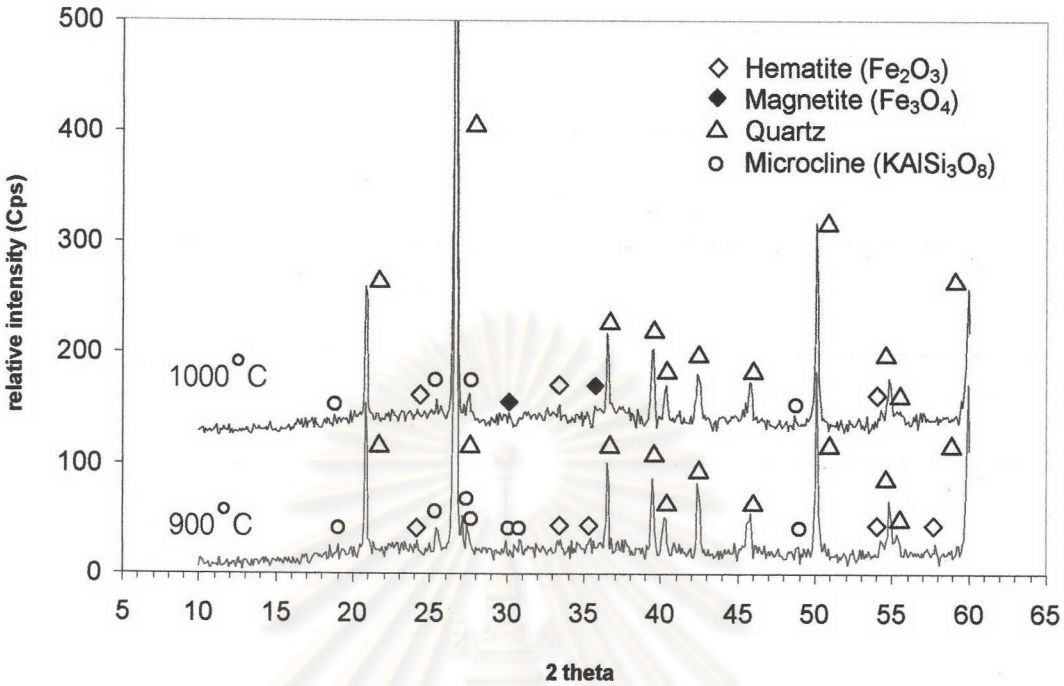

Fig. 4.23. Crystal phases of mixed clay1 fired at 900°C and 1000°C.

4.3.7 Summary

1. The coarse particles of sand and grog disturbed the shrinkage of clay.

2. The effect of particle size of sand on water absorption was small comparing with that of its amount. The effect of particle size of grog on water absorption was large comparing with that of its amount.

3. Fired color of specimen varied from orange to purple and dark-brown color, depending on the firing temperature.

4. Porosity in mixed clay 2 decreased compared with that of mixed clay 1. Fine sand particles also decreased porosity as shown mixed clay 2.

5. Particle size of sand affected the bending strength significantly. The effect of particle size of sand was small comparing with that of its amount. The effect of amount and particle size of grog was not significant as that of sand.

From the above conclusion, water absorption can not be decreased significantly only by changing amount and size of sand and grog. Then we did further experiment by adding more fluxes. The detail is reported in the next chapter.

4.4 Effect of adding flux component

4.4.1 Shrinkage

Fig. 4.24 shows firing shrinkage of composition with fluxing materials compares with standard composition. The firing shrinkage increases at lower temperature by increasing the glassy phase.

The CaO source is $CaCO_3$ and 1 wt% CaO has almost the same effect with adding 6 wt% glass, but lower than 8 wt% glass. Eight wt% glass shows the highest firing shrinkage. The firing shrinkage of 3 wt% NaO was not measured because specimens warped and broke after firing.

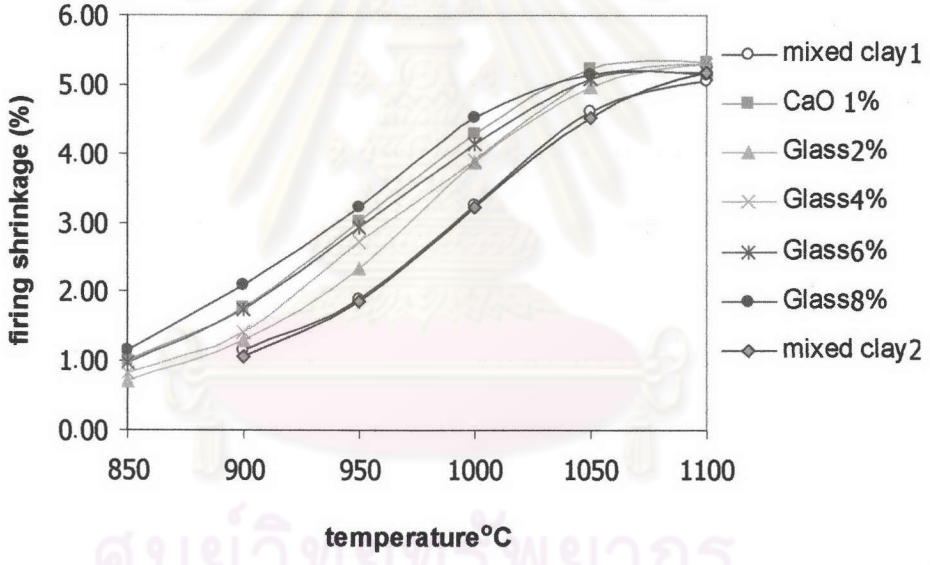

Fig. 4.24. Firing shrinkage of mixed clay1, 2, 1% CaO and glass (2%, 4%, 6%, 8%).

4.4.2 Water absorption and bulk density

Fig. 4.25 (a) shows water absorption of mixed clay 1, 3 wt% NaO and 1 wt% CaO. Water absorption is much reduced significantly when fluxing materials were added. NaO source is $NaCO_3$ (>99.0%, Fluka chemie 71351) and CaO source is $CaCO_3$ (>99.0%, Claymin PCC 2500). $NaCO_3$ shows high efficiency as fluxing material because water absorption of composition with 3 wt% NaO at 850°C is about 11.7%. It is lower than 13.3% of mixed clay 1 at 950°C. Considering from the water absorption, 3 wt% NaO can reduce firing temperature about 100°C.

Water absorptions of 1 wt% CaO at 900 and 950°C are 13.3% and 10.4%, respectively. The values are lower than those of mixed clay 1 firing at 900 and 950°C. Hence $CaCO_3$ is a good flux material, but $CaCO_3$ exothermically decomposes to release carbon dioxide at 899°C (45) and pores were generated, that might increase water absorption if high amount of $CaCO_3$ is added.

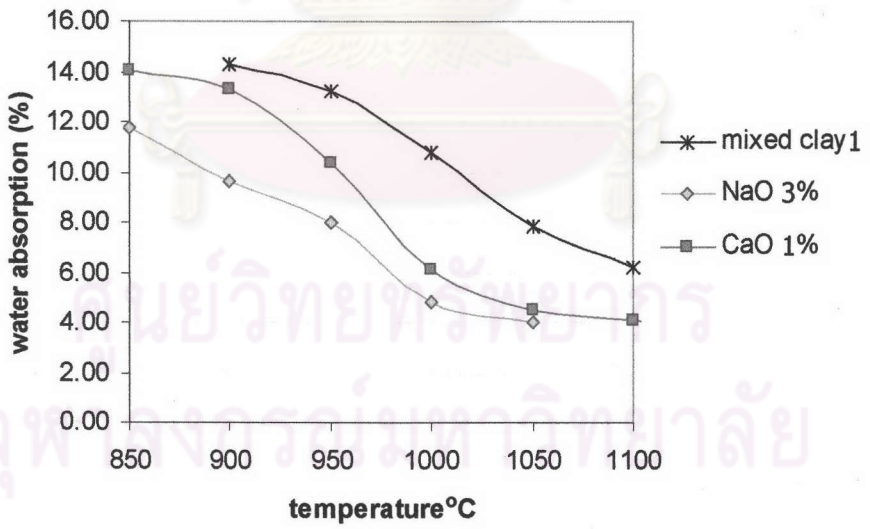

(a)

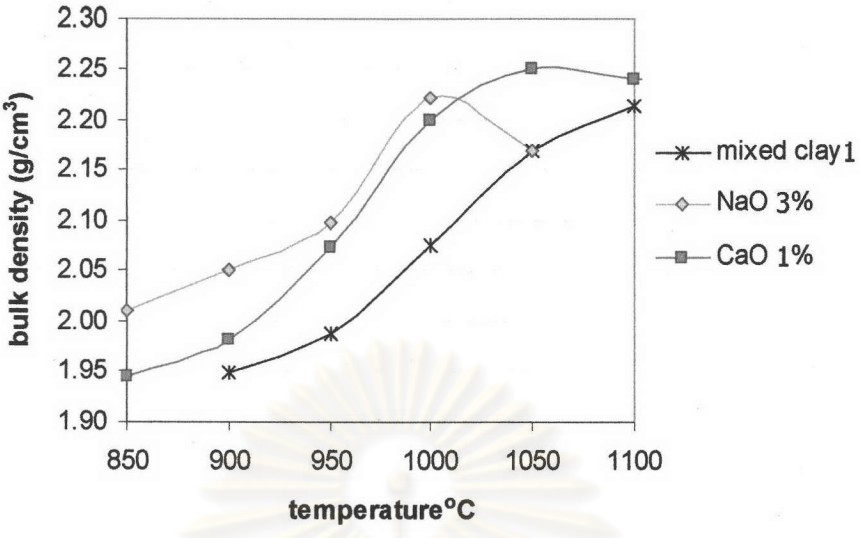

(b)

Fig. 4.25. Water absorption (a) and bulk density (b) of mixed clay1, 3% NaO and 1% CaO.

Fig. 4.25 (b) shows bulk densities of mixed clay 1, 3 wt% NaO and 1 wt% CaO. Bulk density of 1 wt% CaO is higher than that of mixed clay 1 and the same value of bulk density is obtained at temperature 50°C lower than mixed clay 1. In the case of 3 wt% NaO, bulk density becames higher than that of mixed clay 1 and the bulk density shows the same value at firing temperature 100°C lower. But the trend of bulk density drop at high temperature, especially at 1050°C, because the melting point of $NaCO_3$ is 851°C (45) and surface of specimen bloated from boiling bubbles.

Fig. 4.26 (a) shows water absorption of mixed clay1, glass (2%, 4%, 6% and 8%). Soda-lime glass powder is a good fluxing material to reduce the water absorption of mixed clay 1 (original mixed clay). Water absorption decreases significantly with increasing both firing temperature and the amount of glass powder. Water absorption much decreases at lower temperature by increasing the glassy phase. Water absorption of 4% glass at 850°C is lower than that of mixed clay 1 at 950°C.

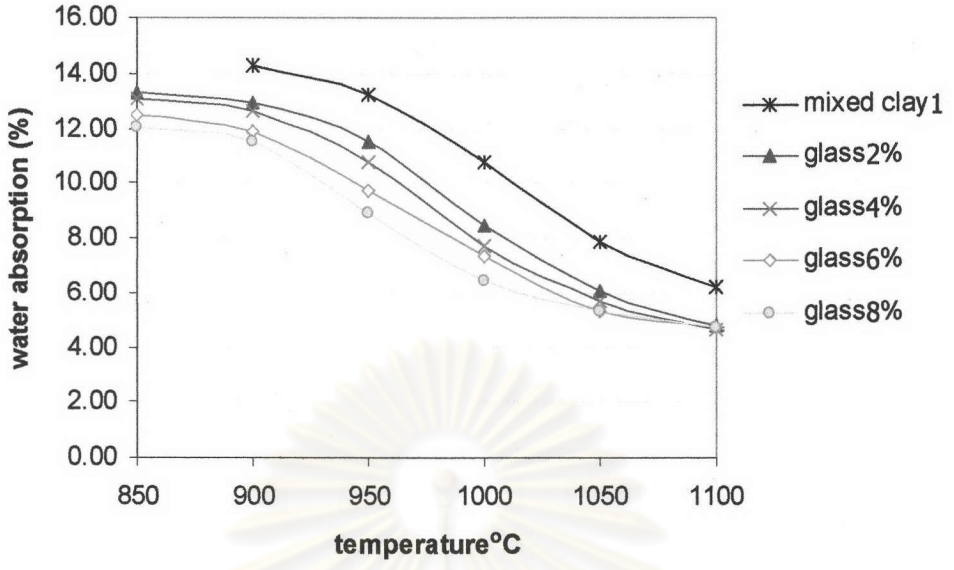

(a)

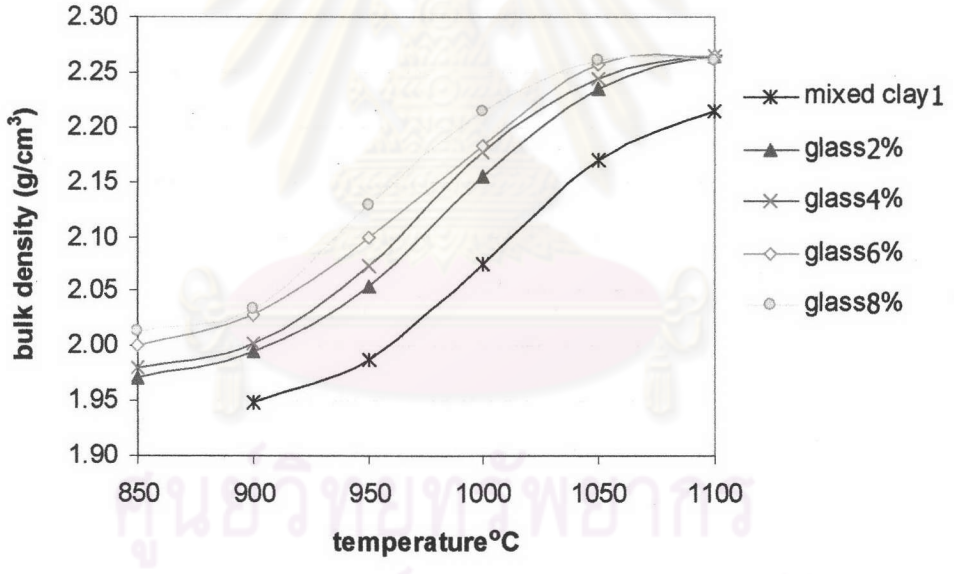

(b)

Fig. 4.26. Water absorption (a) and bulk density (b) of mixed clay1, glass (2%, 4%, 6% and 8%).

Fig. 4.26 (b) shows bulk density of mixed clay1, glass (2%, 4%, 6% and 8%). Bulk density increases with increasing amount of glass. Bulk density of glass 4% at 950°C (about 2.07 g/cm^3) is higher than that of mixed clay 1 (about 1.99 g/cm^3). Comparing with those of Portugal and German products, soda-lime glass powder is a good flux material which decreases water absorption and increases bulk density. 4% of glass can reduces firing temperature about 50-100°C compared with mixed clay 1.

4.4.3 Color

Fig. 4.27 shows fired color of 3 wt% NaO specimens at 850-1050°C. The NaO source is $NaCO_3$ which is soluble in water. When dried, rough surface with white color created. The scum covering the specimen surface was the result of salt deposited. The white color remained on the surface after firing at low temperature about 850-900°C. The specimen warped, the surface bloated and glassy phase generated after firing at high temperature (950-1050 °C).

Fig. 4.27. Fired color of 3% NaO.

Fig. 4.28 shows fired color after adding CaO and glass as fluxes to the specimens fired at 950°C (production temperature). The orange color of hematite occurs at this temperature and these additives do not show significant difference in fired color. Because soda-lime glass powder has low percentage of FeO (0.09 wt.%). Calcium silicate is white in color but if it becomes major phase, it will expel ferric oxide into grain boundaries and show points of hematite concentration. (23)

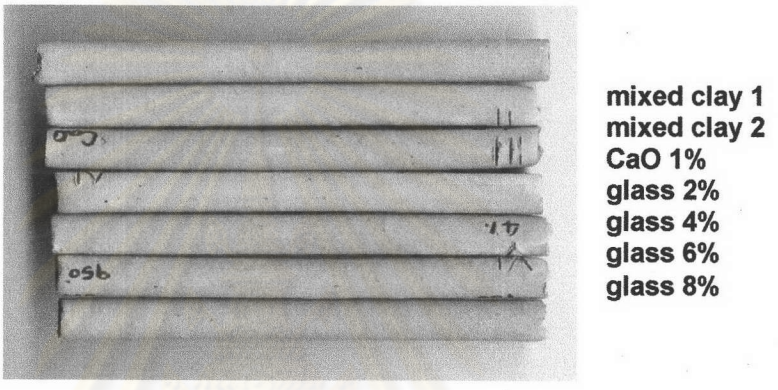

Fig. 4.28. Fired colors of specimens with CaO and glass fluxes sintered at 950°C.

4.4.4 Microstructure

Fig. 4.29 shows cross sectional microstructures of 1 wt% CaO specimens. Coarse sand particles are present inside the body but the porosity from shrinkage of the mixture components is reduced significantly because CaO acts as flux to produce glassy phase for binding particles together. The porosity from an ineffective pressing is present at high temperature but in less amount than those of mixed clay 1 and 2. In the specimens fired at 1050-1100°C, dark-brown color area is shown because calcium silicate expels ferric oxide into grain boundaries. (23)

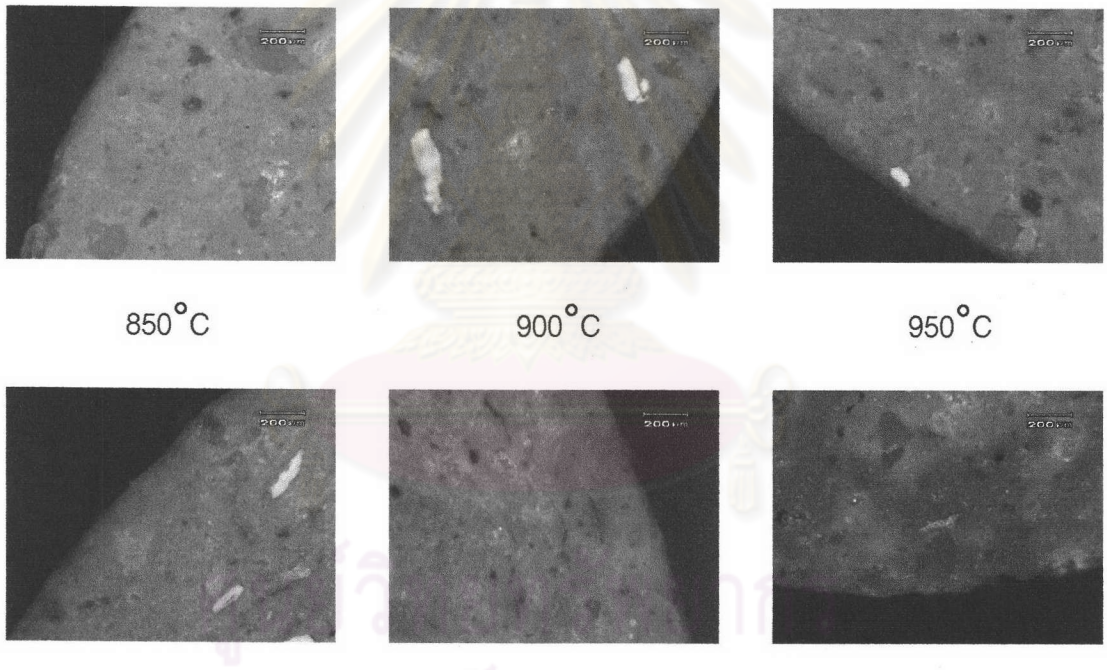

Fig. 4.29. Cross sectional microstructures of 1% CaO specimens.

Fig. 4.30 shows cross sectional microstructures of 4 wt% glass specimens. Coarse sand particles are present but the porosity from shrinkage of the mixture components and from the ineffective pressing are reduced less than those of mixed clay 1 and 2. Because soda-lime glass powder acts as a flux material, it increases glassy phase to reduce the porosity and close particles together. Because calcium silicate in soda-lime glass expels ferric oxide into grain boundaries, dark area generates in the specimen sintered at high temperature about 1050-1100°C.

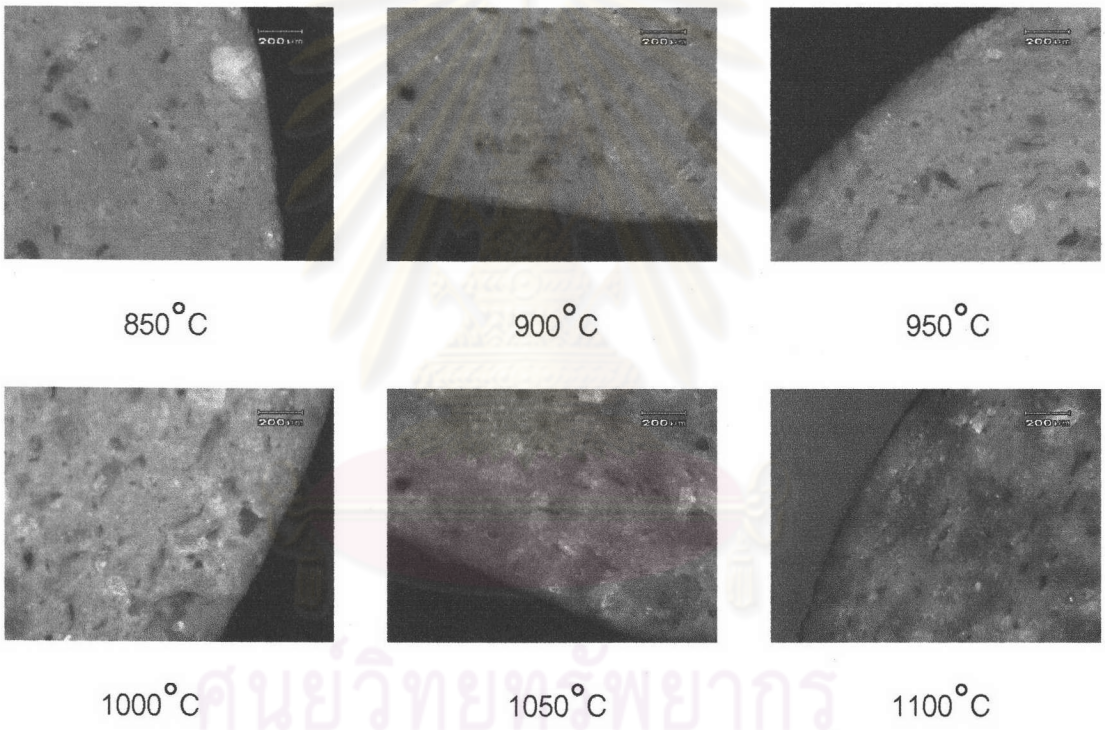

Fig. 4.30. Cross sectional microstructures of 4% glass specimens.

4.4.5 Bending strength

Fig. 4.31 shows three point bending strength of mixed clay1, 3% NaO and 1% CaO specimens. Bending strength of 1% CaO is higher than mixed clay 1 at every temperature. In the case of 3% NaO, despite water absorption is lower and density is higher than those of mixed clay 1, its bending strength is very lower than that of mixed clay 1. Because Na_2CO_3, as the source of NaO starts to melts at 851°C and boils at higher temperature, then the strength of specimen is decreased.

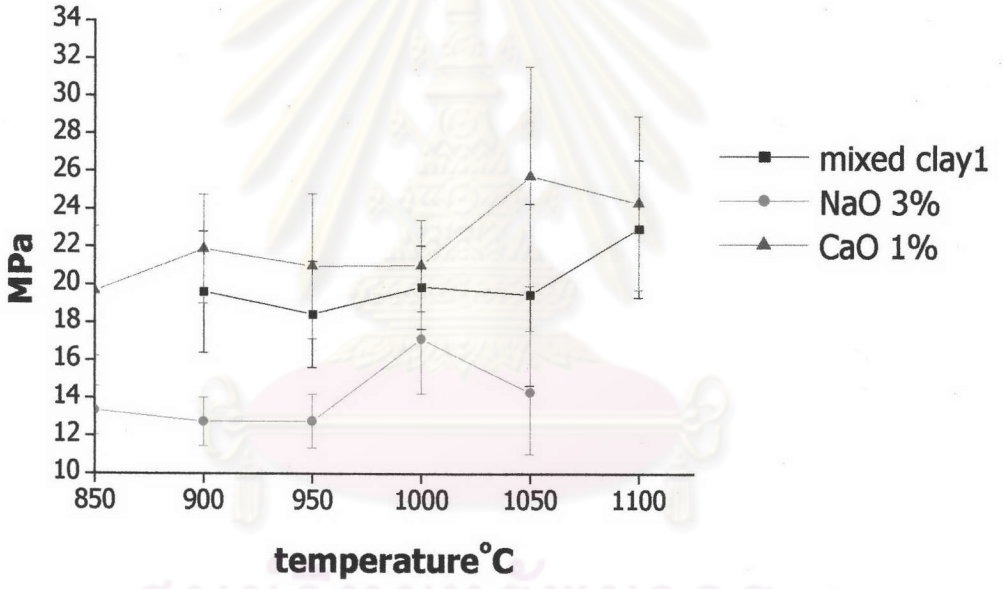

Fig. 4.31. Three points bending strength of mixed clay1, 3% NaO and 1% CaO.

Fig. 4.32 shows three point bending strength of mixed clay1, glass (2%, 4%, 6% and 8%) specimens. Bending strength of specimens with glass increases, but the increment does not depend on the amount of glass. As a result, adding 2 wt.% of glass is enough to raise the strength of the standard (mixed clay 1).

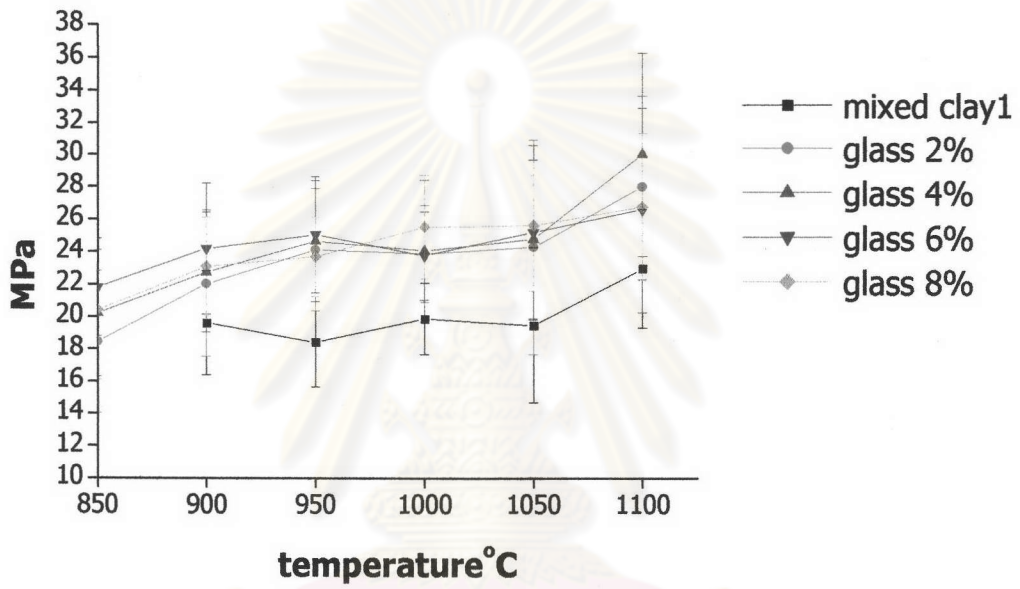

Fig. 4.32. Three points bending strength of mixed clay1, glass (2%, 4%, 6% and 8%).

4.4.6 Crystal phase

Fig. 4.33 shows XRD patterns of 1% CaO fired at 900°C and 1000°C. Quartz is the main phase presented at both temperatures. Hematite and microcline are presented at 900°C which is the same as mixed clay 1. At 1000°C, Magnetite presented and pseudowollastonite ($3CaSiO_3$) occurs because calcium carbonate reacts with silica. The reaction starts after the carbonate decomposed (46) according to equation (1), (2) and (3).

$$2CaO + SiO_2 \rightarrow Ca_2SiO_4 \quad \text{---------- (1)}$$

$$3Ca_2SiO_4 + SiO_2 \rightarrow 2Ca_3Si_2O_7 \quad \text{---------- (2)}$$

$$Ca_3Si_2O_7 + SiO_2 \rightarrow 3CaSiO_3 \quad \text{---------- (3)}$$

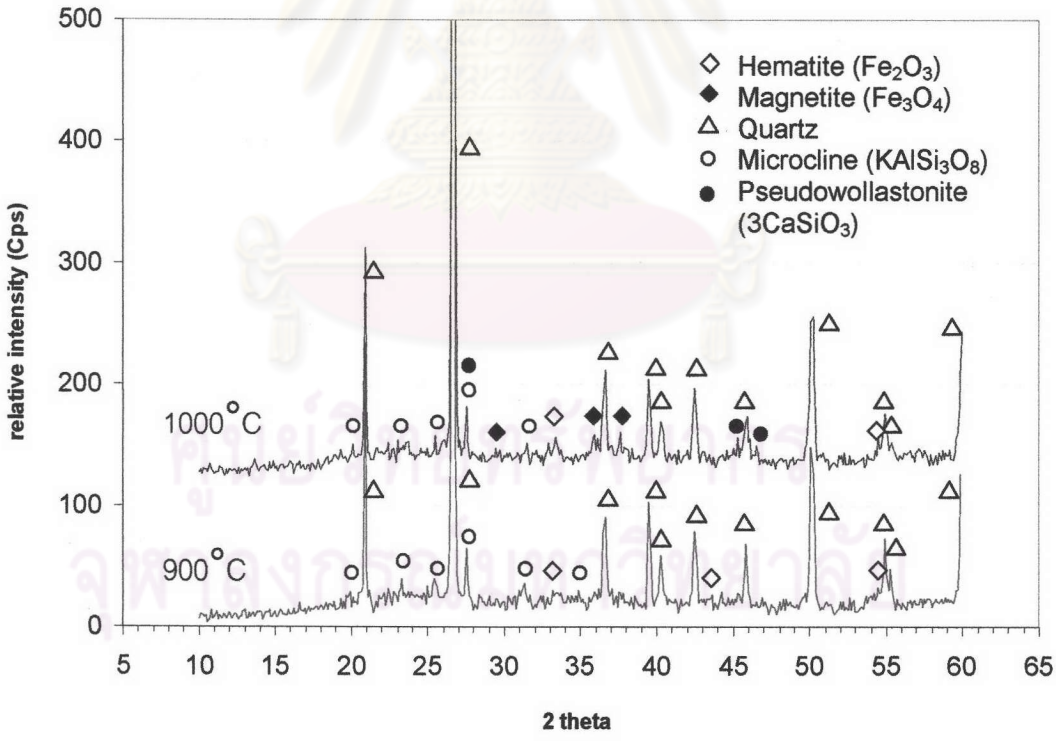

Fig. 4.33. Crystal phase of 1% CaO fired at 900°C and 1000°C.

Fig. 4.34 shows XRD patterns of 8% glass fired at 900°C and 1000°C. Quartz is the main phase presented at both temperatures. Hematite and microcline are presented at 900°C same as in mixed clay 1. Albite (sodium aluminum silicate) is presented at 900°C because soda-lime glass includes high percentage of NaO. At 1000°C, the content of hematite phase which is the origin of orange color is reduced and a little amount of magnetite phase occurs. Calcium sodium iron aluminum silicate presented at 1000°C because soda-lime glass includes high percentage of CaO.

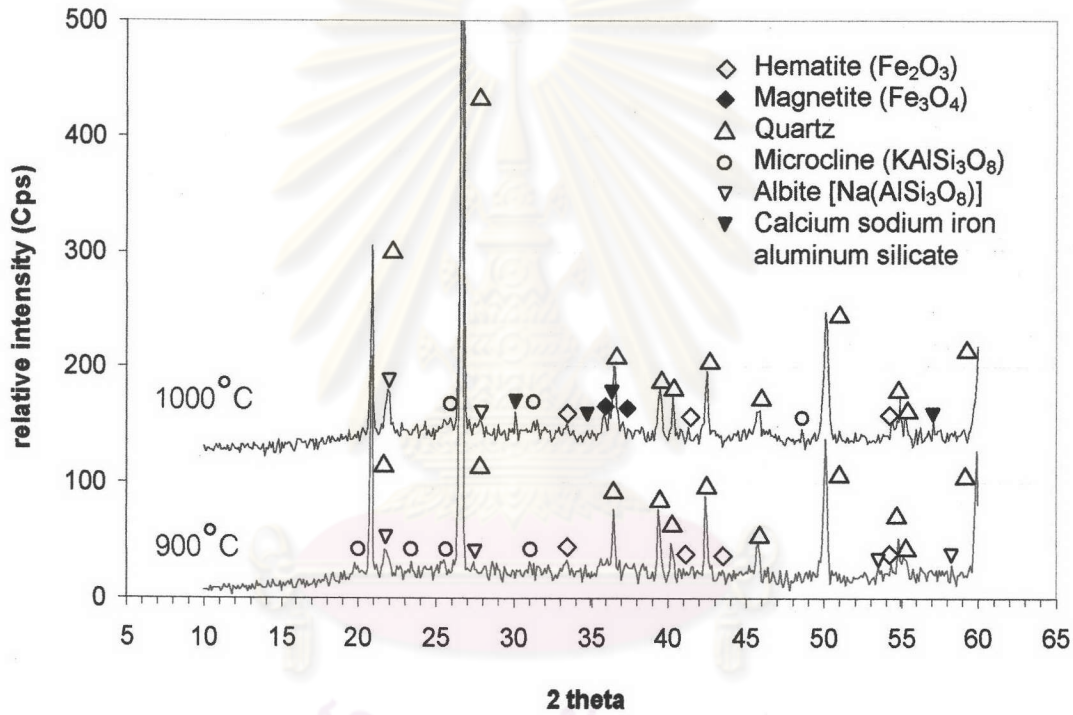

Fig. 4.34. Crystal phase of 8% glass fired at 900°C and 1000°C.

4.4.7 Summary

1. The firing shrinkage increased at lower temperature by increasing the glassy phase.

2. Water absorption decreased and bulk density increased significantly with adding flux materials.

3. The orange color of hematite occurred at 950°C and each flux shows no significant difference in fired color, except NaO.

4. Coarse sand particles were presented in microstructure of 4% glass but the porosity from shrinkage of the mixture components and from the ineffective pressing were reduced.

5. Bending strength of specimens with adding of flux component increased.

Concerning all properties, it was concluded that adding 4-6 wt% of glass powder was effective to decrease water absorption and increase bending strength.

4.5 Experimental result at factory

4.5.1 Shrinkage

Fig. 4.35 shows firing shrinkage of mixed clay1, S50G5 and SGG compositions. Mixed clay 1 contains 5 wt% of sand including coarse particle and 8 wt% of grog. S50G5 is an optimal formula with no flux added which contains 5 wt% of sand 50 mesh and 5 wt% of usual grog. The particle size of grog was not reduced because it did not show large effect on properties. Grog is a scarce material in the future. The amount of grog is decreased because the resource of grog is reduced in the future by the improvement of production. The firing shrinkage of S50G5 is a little higher than that of mixed clay1 at temperature above 950°C. SGG is the material same as S50G5 but with a flux material (5 wt% of glass powder) added. The firing shrinkage of SGG increases at a temperature lower than 1050°C.

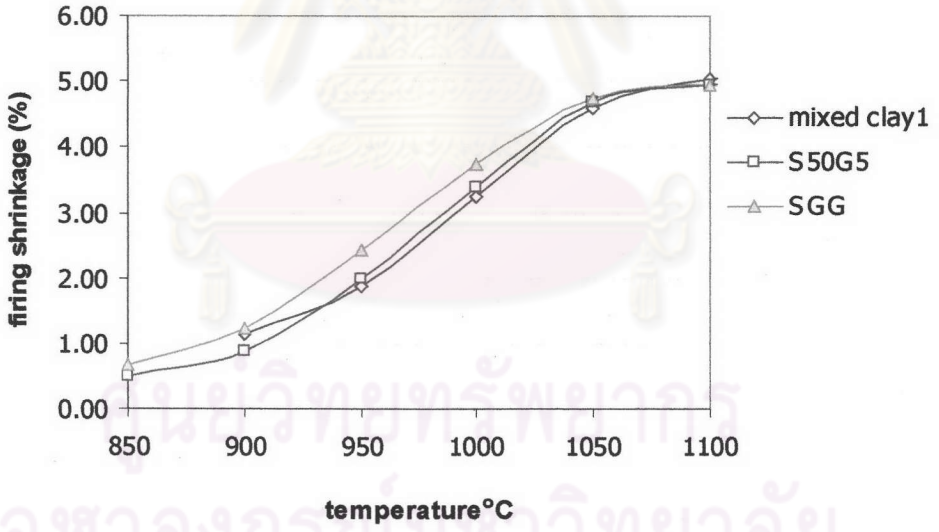

Fig. 4.35. Firing shrinkage of mixed clay1, S50G5 and SGG.

4.5.2 Water absorption and bulk density

Fig. 4.36 (a) shows water absorption of mixed clay 1, S50G5, and SGG specimens. Water absorption of SGG at 950°C decreases to 9.6% compared to the 13.6% of standard mixed clay 1.

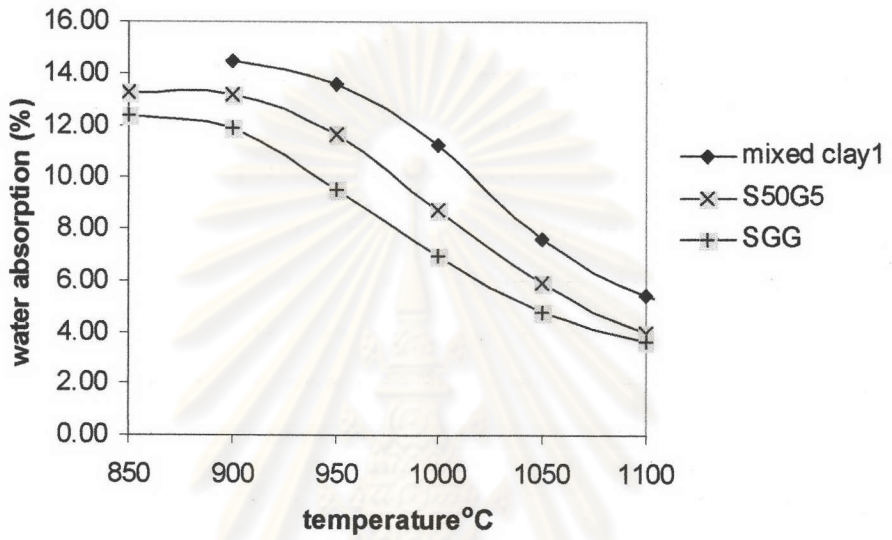

(a)

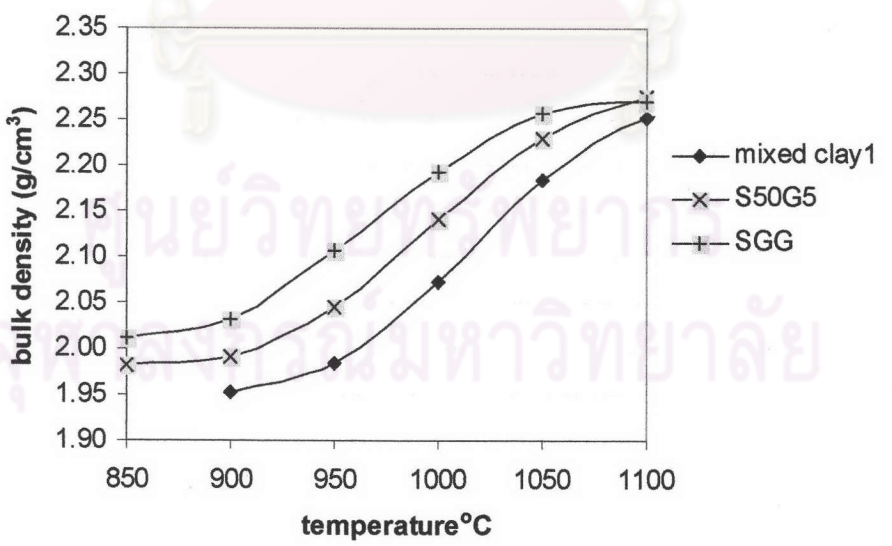

(b)

Fig. 4.36. Water absorption (a) and bulk density (b) of mixed clay1, S50G5 and SGG specimens.

Fig. 4.36 (b) shows bulk densities of mixed clay1, S50G5 and SGG specimens. Bulk density of SGG at 950°C (about 2.01 g/cm^3) is higher than that of mixed clay 1 (about 1.98 g/cm^3). Bulk density of SGG is intermediate, between mixed clay 1 and SGG.

Fig. 4.37 shows water absorption of S50G5 and SGG comparing with commercial products. Water absorption of SGG1 is 11.8% and SGG2 is 11.9%. The water absorption of SGG is lower than that of Portugal. The water absorption of S50G5 is similar with that of Portugal.

In the form of test piece, water absorption of SGG at 950°C is about 9.6% as shown in Fig. 4.36 (a). It is lower than that of German product (about 9.7%). The firing temperature of gas furnace is in the range of 900-950°C. Therefore, the SGG pottery might be fired around 900°C.

Fig. 4.37 (b) shows water absorption in each part of products of S50G5 and SGG comparing with commercial ones. The trends of water absorption of S50G5 and SGG are the same as those of SM and Portugal commercial products.

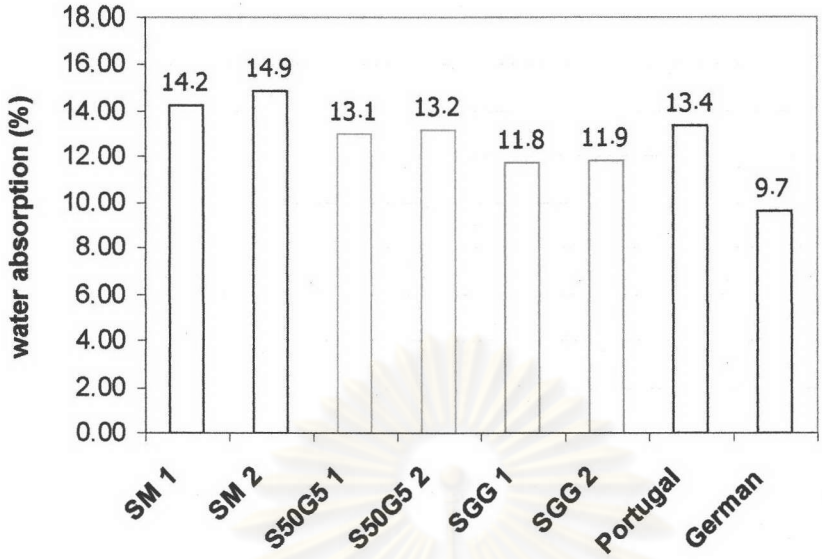

(a)

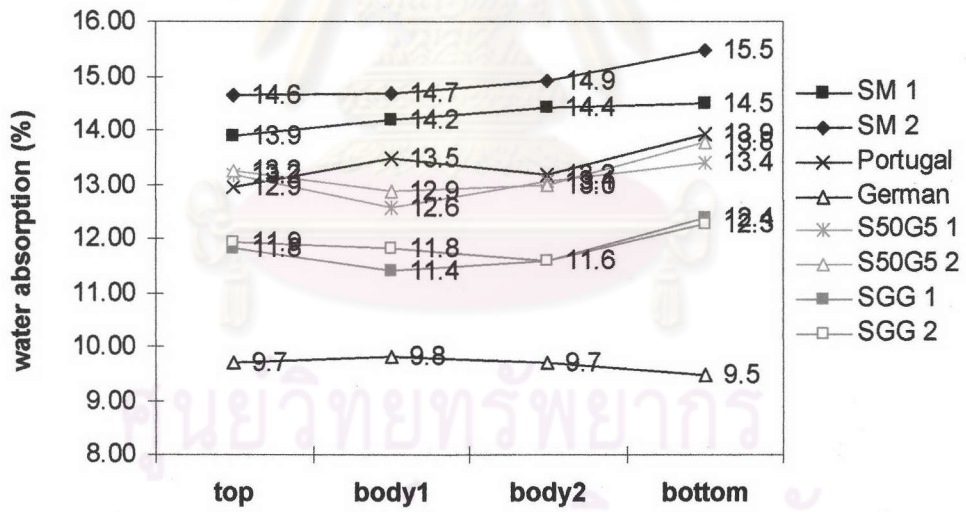

(b)

Fig. 4.37. Water absorption of S50G5 and SGG compared with commercial products (a) average water absorption, (b) each part of products (SM = Siamese Merchandise Co.,Ltd., 1=small size (top diameter = 19 cm), 2=large size (top diameter = 32 cm)).

Fig. 4.38 (a) shows average bulk densities of S50G5 and SGG comparing with commercial products. Bulk density of SGG 1, 2 (about 2.02 g/cm^3) is higher than S50G5 1 (about 1.99 g/cm^3), S50G5 2 (about 1.98 g/cm^3), SM 1 (about 1.95 g/cm^3), SM 2 (about 1.93 g/cm^3) and Portugal product (about 1.95 g/cm^3), but lower than German product (about 2.12 g/cm^3).

Fig. 4.38 (b) shows bulk density in each part of products of S50G5 and SGG comparing with commercial products. The trends of water absorption of S50G5 and SGG are the same as those of commercial products.

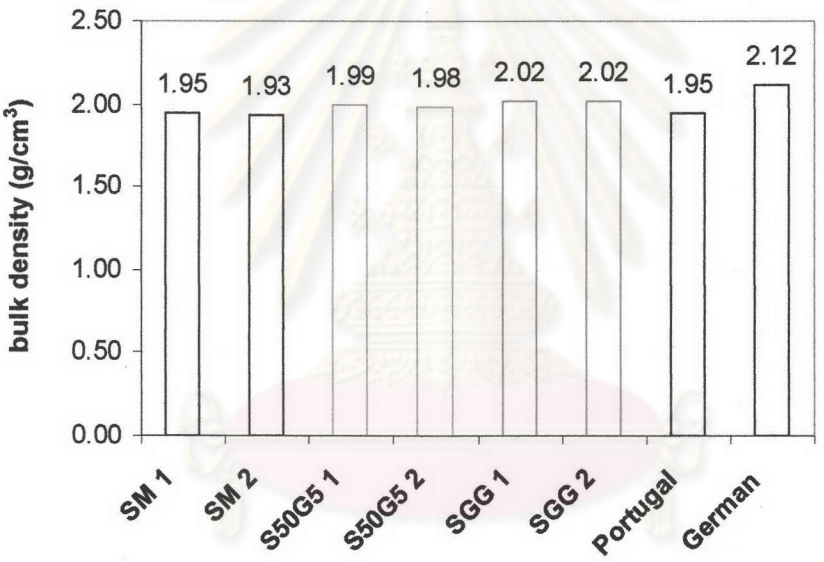

(a)

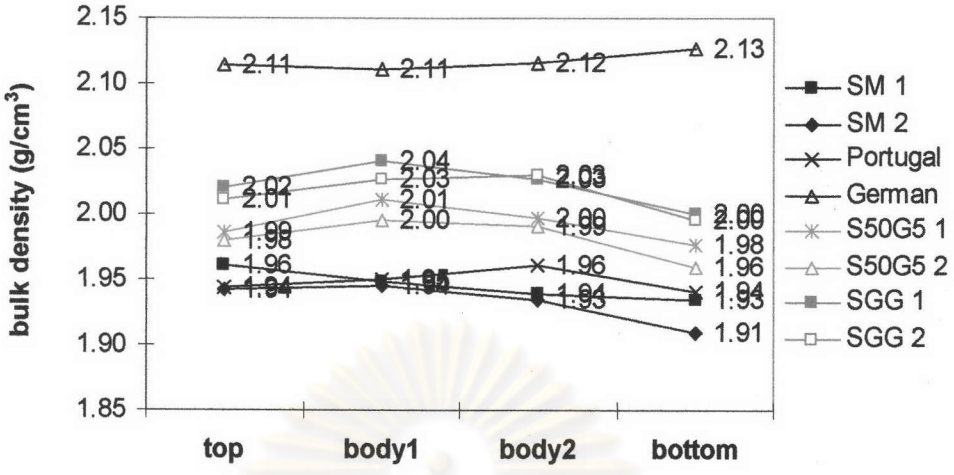

(b)

Fig. 4.38. Bulk density of S50G5 and SGG compared with commercial products (a) average bulk density, (b) each part of products (SM = Siamese Merchandise Co.,Ltd., 1=small size (top diameter = 19 cm), 2=large size (top diameter = 32 cm)).

4.5.3 Capillary pore volume

Fig. 4.39 shows capillary pore volume (< 2 μm) of S50G5 and SGG products compared with commercial products. The frost damage is induced from the freezing of entrapped water in capillary pore. Therefore, low capillary pore volume is essential for high frost resistance property. The capillary pore volumes of Portugal and German products are very low, while the capillary pore volumes of SM 1 (about 0.082 ml/g), SM 2 (about 0.090 ml/g) and S50G5 products (about 0.084 ml/g) are large. However, it decreased to the similar level with Portugal when SGG was sintered at 950°C.

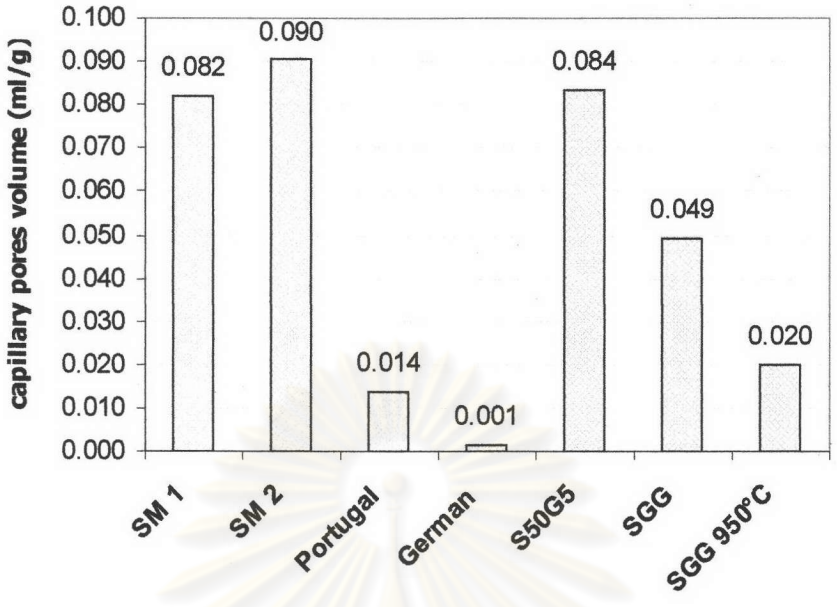

Fig. 4.39. Capillary pore volume (< 2 μm) of S50G5 and SGG compared with commercial products.

4.5.4 Microstructure

Fig. 4.40 shows microstructures of experimental products. Fine sand particles are presented at the inside of the body because coarse sand particles are removed from both of S50G5 and SGG products. In the case of S50G5, the porosity is reduced significantly and the porosity from the ineffective pressing still remains but is less than the SM product. Soda-lime glass powder about 4.8% in SGG decreases the porosity from the shrinkage of the mixture components while porosity from the ineffective pressing is still present, but the amount is less than that of SM and S50G5 product.

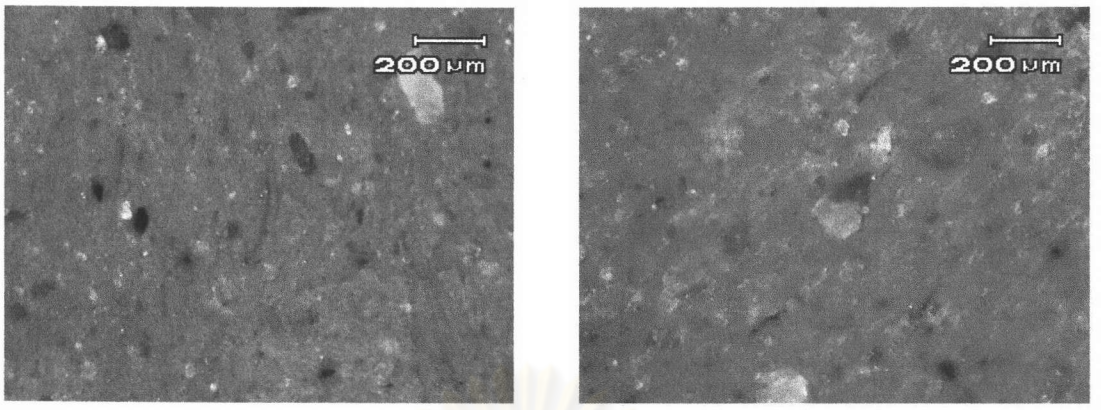

(a) (b)

Fig. 4.40. Microstructures of experimental products (a) S50G5 and (b) SGG.

4.5.5 Bending strength

Fig. 4.41 shows three point bending strength of mixed clay1, S50G5 and SGG specimens. From the high bulk density and low water absorption, higher bending strength in SGG specimen is expected. However, bending strength of SGG is not higher than those of S50G5 and mixed clay 1 significantly. Low bending strength might come from air void inside specimens because the extrusion operation was performed without vacuum system and a coarse particle might be present at breaking point of specimen.

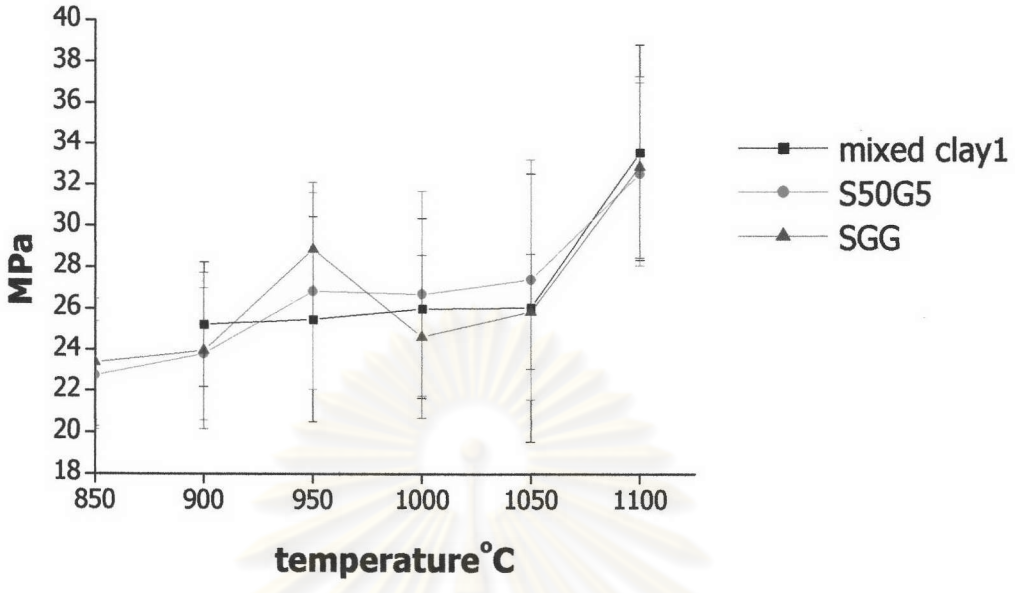

Fig. 4.41. Three points bending strength of mixed clay1, S50G5 and SGG.

4.5.6 Freeze-thaw testing (DIN 52252 standard method)

Each one of the SGG pottery samples, small size (190 mm diameter x 170 mm height) and large size (320 mm diameter x 270 mm height), were tested. The damage of samples were examined visually for after 12th freeze-thaw cycle and at the end of the test (25 times). The purpose of this standard, frost damage test is to observe damages, such as cracking and flaking, by the naked eye.

All of the samples passed the test after 25 freeze-thaw cycles. There were no sign of damage in the form of cracking and flaking.

4.5.7 Summary

1. Firing shrinkage increased at lower temperature by increasing the glassy phase in SGG composition.

2. Water absorption of S50G5 was significantly lower than mixed clay 1 at every temperature and water absorption of SGG was also lower than that of S50G5 at every temperature.

3. Capillary pore volume (< 2 μm) of SGG product decreased to lower than that of SM commercial products, but was still higher than those of Portugal and German commercial products. However, the capillary pore volume of SGG decreased to the similar level with that of Portugal, when it was fired at 950°C.

4. The porosity from the shrinkage of the mixture components and the ineffective pressing decreased in SGG composition.

5. Bending strength of SGG was not higher than S50G5 and mixed clay 1 significantly.

6. All of SGG pottery samples survived the test after 25 freeze-thaw cycles according to DIN 52252 standard method. They showed no sign of damage in the form of cracking and flaking.

As a result, the properties of SGG were better than that of SM in total.